Hochschule für Angewandte Wissenschaften Hamburg

Fakultät Life Sciences

Design and Development of a MRI and U.S. Compatible Heart Phantom

Master Thesis

Presented by

Manan Patel

2055748

Submitted on July 22, 2013

Supervisor:	Prof. Dr. Ing. Friedrich Ueberle	HAW Hamburg
Supervisor:	M. Sc. Fabian Kording	Universitätsklinikum Hamburg-Eppendorf

The thesis was supervised and created in the department of Biomedical engineering at HAW Hamburg, Bergedorf and Department of Diagnostic and Interventional Radiology at Universitätsklinikum Hamburg-Eppendorf

<u>Declaration</u>

I understand the nature of plagiarism, and I am aware of the University's policy on this. I hereby declare that this thesis report presents original work done by me, excepts resources used with their reference. All used resources are explicitly referenced in the Bibliography.

X
_____
Manan Patel

Abstract

Development of techniques for fetal magnetic resonance imaging are extremely useful for prenatal diagnosis. One such technique uses Ultrasound Doppler cardiotocography signal of fetal heart for triggering magnetic resonance imaging system. Refinement of an triggering algorithm requires testing on living pregnant test subjects(humans or animals). Steady supply of such test subject is not feasible. A midway solution is needed which can help in initial testing of an algorithm and then moving forward to testing on live subjects.

Since the target organ is fetal heart, development of a heart phantom can be an excellent solution to meet demands for test subject. A dynamic heart phantom which can provide sufficient Doppler signal for triggering will help in testing of accuracy and precision of a triggering algorithm.

A rubber water balloon was placed in a closed acrylic chamber and filled with water. The balloon was forced to inflate-deflate periodically with the help of external suction force and elastic property of the rubber balloon. The amount of suction was controlled using a control box, operating outside gantry room.

Testing under 1.5T magnetic resonance imaging system showed that signals from phantom could be successfully used for triggering of the imaging system. Also visible changes in the internal area of balloon in each cross sectional slice were obtained till 133 beats per minute operation. Important parameters relating to a heart's function, like stroke volume, flow rate, flow velocity were calculated using images of phantom. Attempts were made to gather data using USD for correlation of calculated parameters using MRI image processing. After careful study of the results and performance of phantom, it was concluded that a more realistic model of heart phantom could be developed with further refinement in current design.

Contents

List of Figures

List of Tables

List of Abbreviations

AFECG	Abdominal Fetal Electrocardiogram
AV	Atrio-Ventricular
AV	Atrio-ventricular
bpm	beats per minute
bpm	beats per minute
cMRI	Cardiac Magnetic Resonance Imaging
CTG	Cardiotocogram
C.T.	Computed Tomography
ECG	electro cardiogram
ECG	electrocardiogram
IUGR	Intra-Uterine Growth restriction
LV	left ventricle
MRI	Magnetic Resonance Imaging
NMR	Nuclear Magnetic Resonance
PVAc	Poly Vinyl Alcohol Cryoge
PVA	Poly Vinyl Alcohol
Rf	radio-frequency
SNR	signal-to-noise ratio
S.V.	Solenoid Valve
USD	Ultrasound Doppler imaging device
V.P.	Vacuum Pump

1 Introduction

1.1 Background and Context

Nuclear Magnetic Resonance (NMR) imaging or Magnetic Resonance Imaging (MRI) is a very resourceful imaging modality. In MRI powerful magnets and radio-frequency (Rf) signals are used to reconstruct internal structure of an object non-invasively. With the help of MRI we can see cross-sectional view of any part of body at any desired axis (1). Another Imaging modality offering similar feature is X-ray Computed Tomography(C.T.). In C.T. high energy X-ray radiation is made to penetrate desired segment of body. Usage of X-ray has a disadvantage that it uses high energy X-ray radiation, which has ionizing effect on tissue. Both X-ray Computed Tomography and MRI are non invasive procedures, however usage of magnetic fields and Radio-frequency (Rf) pulses has no ionizing effect on target tissue. This particular feature of MRI makes is more recommended in many studies.

Cardiac Magnetic Resonance Imaging (cMRI) is a procedure for studying heart. With the help of MRI one can study Heart's structure, Heart's functionality. As mentioned above its very important that the test subject, in this case the Heart, remains stationary (motionless) while the data for image reconstruction are obtained; however, heart is not a stationary organ. As long as subject is alive it keeps beating. Its beating movement and blood flow makes it really hard to get images with good contrast. A study of abnormality in its anatomical structures, physiological activity is hindered because of lack of images with good contrast. To achieve this requirement special techniques have been developed which help in getting sharp images with good contrast. One of the technique used is breath-hold technique. In this technique Patient is asked to hold his/her breathe during data acquisition. This methods produces good results; however, the procedure time is very lengthy. Another techniques requires synchronization with electrocardiogram (ECG) signal (2). In this technique data acquisition phase is synchronized with heart rhythm. With the help of Cardiac MRI it is possible to study cardiac indications and diseases. For e.g. Coronary heart disease, Damage caused by a heart attack, Heart Failure, Congenital heart defects(heart disease present at birth), Pericarditis(a condition in which the membrane, or sac, around heart is inflamed), Cardiac tumours, etc.

Cardiac MRI becomes an easy procedure to carry out in case of adults because the ECG signal, which is the fundamental requirement, for synchronization is easily obtainable.

But in case of fetal heart it is almost impossible to obtain ECG signal (3). Prenatal Heart diagnosis is of huge importance because fetal heart malfunctions is the major reason for high mortality and morbidity (4). Ultrasound Sonography is an another modality of imaging for diagnosis. For years it is been considered to be the golden standard for diagnosis. But it has its own limitations. Maternal obesity limits visibility of fetal heart structure to a great extent, as much as 49.8% (5). There are other issues like fetal orientation and scars from previous surgeries (4). All these limitations with Sonography could be overcome with the help of MRI procedure, if there exists a way to sync MRI image data acquisition triggering with fetal heart rhythm. With the help of this technique we can have high quality fetal heart images for diagnosis. A group has come up with a solution. A Ultrasound Doppler device has been modified to make it compatible with MRI (6). Using this Cardiotocogram (CTG) fetal heart Doppler signals are gathered, processed and then used for triggering MRI for image acquisition (3). As a result good sharp images were obtained as shown in Figure 1.1 (7).

The process of Doppler signal processing and generating trigger signal for MRI is still under development phase. While development process continues a constant supply of test body is required. Since the test target is fetal body it is highly inconvenient to arrange a constant supply of test bodies, both human volunteers as well as animal sources. A convenient solution to this problem is to use a phantom. A phantom will help in initial testing and verification of a signal processing algorithm.

A phantom has an advantage that it almost replicates real life like scenario of test subject. Therefore initial testing and verification of an idea can be performed on a phantom and then we can move forward for testing it actual test subject. Another advantage of having a phantom is it helps in reducing development cost and which can mimic ventricular action of a heart with periodic rhythm and visible volumetric changes.
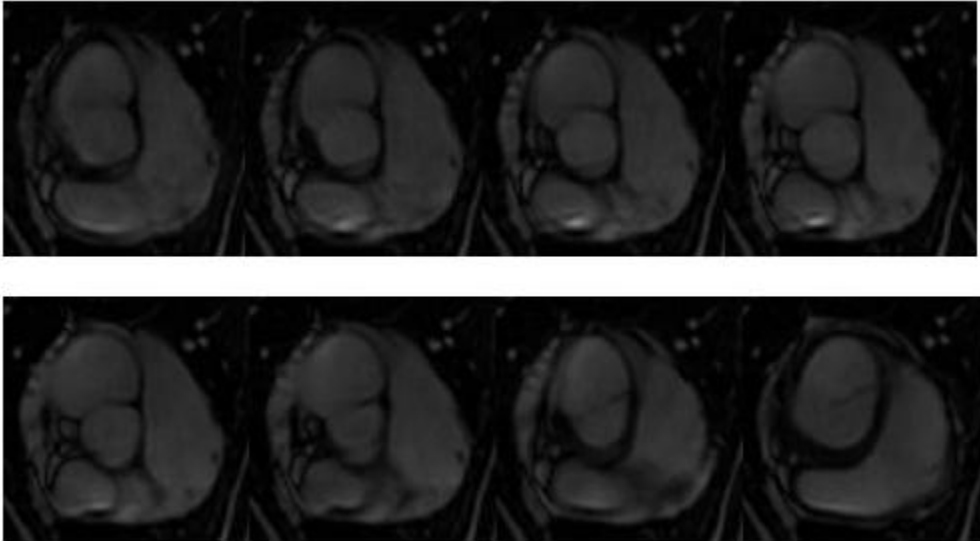
Figure 1.1 Comparison of MRI frames of a cine sequence of sheep fetal heart without Ultrasound triggering(above) and with Ultrasound Triggering(below) (7).

1.2 Scope and objectives

In present work, after analysing design and operating principles various phantom available commercially and non-commercially, we try to design and develop a phantom for Fetal heart. This phantom should meet following requirements:.

1. Operating range of about 180 beats per minutes
2. Sufficient stroke volume at high operating frequency
3. Should provide sufficient frequency shift in Ultrasound for detection by Doppler device.
4. MRI compatible.

Phantom will be tested with the help of MR system for its working at different beats per minute (bpm) settings and with Ultrasound Doppler imaging device (USD) to study flow pattern and flow velocity. From MRI images we calculate balloon's stoke volume, flow velocity and flow rate of fluid with the help of MRI images and compare calculated results with results obtained using USD.

1.3 Achievements

Test results from magnetic resonance imaging system showed that signals from phantom could be successfully used for triggering of the imaging system. Visible changes in the internal area of balloon in each cross sectional slice were observed. Comparison of results, calculated using MRI images and measured with Ultrasound Doppler imaging device, could not be performed because of aliased signal obtained by the USD. Some good recordings are higher beats per minute settings were made but it required manipulation in amount and duration of suction force applied on balloon.

1.4 Overview

In the following chapters we first study and analyse various phantom designs proposed already by various groups. And explain and idea for developing this heart phantom.

Third chapter describes physiology of fetal circulation, fundamentals of MRI and methods of cardiotocography, Cardiotocography,.

In fourth chapter an explanation on various ideas used for developing a heart phantom are explained followed by construction technique and materials used for the phantom to be MRI compatible.

In Fifth and Sixth chapter we describe testing method used for testing the phantom under MRI and USD respectively. Results gathered using this tests are also described in their respective chapter.

Finally we discuss, various aspects of relating to development of a phantom, issues faced, interpretation of results, and points for future developments followed by conclusion of thesis work.

2 State of the art

A good range of heart phantoms are available commercially and numerous phantom designs, physical and numerical, have been proposed by various groups (8) (9) (10) (11) (12) (13) (14) (15), to meet specific requirements. Phantoms could be stationary and dynamic type in action. Along with design ideas, numerous materials such as Agarose and Poly Vinyl Alcohol (PVA) have been proposed as best suitable material for design and development of such phantoms (16) (17) (18). These materials are able to mimic actual tissue properties under MRI to great extent. Few examples of such commercial and non-commercial heart phantoms are as follows:

a) Dynamic Cardiac Phantom
b) Ultrasound Heart Phantom CIRS 067
c) Dynamic Multi-modality Heart Phantom.
d) Rodent Cardiac Phantom.

a) Dynamic Cardiac Phantom:

It is an example of Dynamic type Heart Phantom (19). It is proved to be useful in testing and verification in Nuclear medicine. It simulates left Ventricular operation. Its operation is controlled with the help of a computer with operating frequency of 60 cycles per minutes. The fetal heart operates at about 120-160 (20) beats per minute(bpm). So this phantom is not enough for testing and verification of an algorithm.

Figure 2.1 Dynamic cardiac phantom simulating left ventricle , capable of operating at 60 bpm (19).

b) Ultrasound Heart Phantom CIRS 067:

Its an example of stationary type of heart phantom (21) and its commercially available. Stationary heart phantoms are not suitable for development of Doppler Ultrasound triggering technique because Doppler signals are difficult to generate with stationary object.

Figure 2.2 Ultrasound heart phantom CIRS 067 with complete heart like structure (21).

c) Dynamic Multi-Modality Heart Phantom:

It's an example of dynamic heart phantom and is commercially available (22). It's a pneumatically controlled phantom. It shows an excellent anatomical and physiological similarity to that of real human heart. MRI compatible version of phantom can operate at up to 200 beats per minute. This phantom has two important parts. One is the mould and second is driving mechanism. A two chamber(biventricular) heart mould is produced with the help of actual heart (23). Poly Vinyl Alcohol(PVA) is used to fabricate biventricular heart structure. And is placed in a water filled acrylic chamber. A multi axial servo actuator is attached at one end of the result heart structure. The operation is controlled with the help of software running on a computer.

Figure 2.3 Dynamic heart phantom for multi-modal testing (22). Capable of operating at 200 beats per minute.

d) Rodent Cardiac Phantom:

It's a phantom design for simulating operation of a rodent left ventricle. The design was proposed by a group of researchers at University of Oxford and University of Edinburg (8). Test results show that it can operate at about 240 bpm.
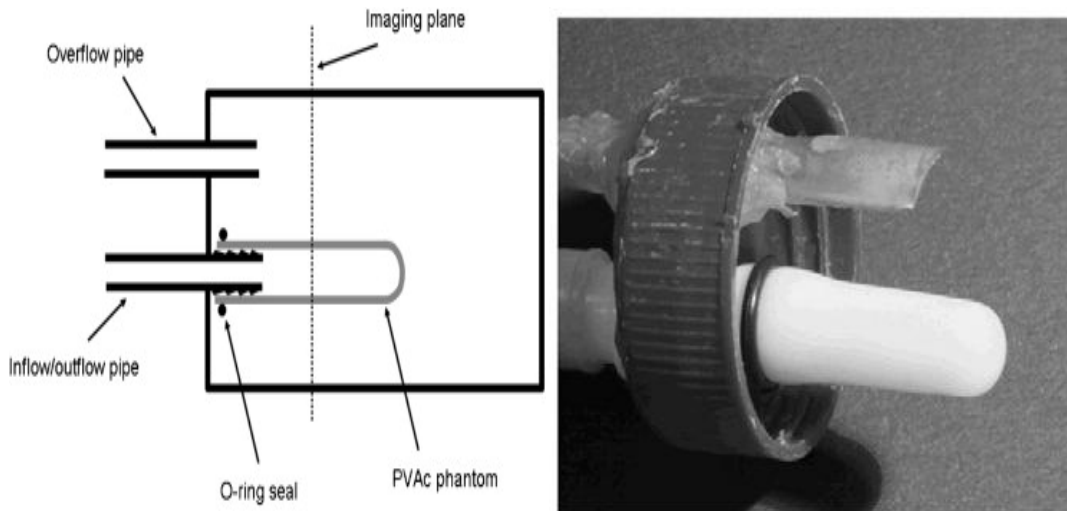
Figure 2.4 Schematic design of a rodent heart phantom(left) and picture of a rodent heart phantom after fabrication (8).

Poly Vinyl Alcohol Cryogel (PVAc) used is to make a shack like structure using a test tube mould. So that it can look as much similar to that of Left ventricle. This mould is fitted over a inflow/outflow tube and fitted in a sealed container filled with water. A pump is used to pump fluid inside phantom, which is operated remotely. Fluid is pumped in and out of sac periodically using a pump operating outside MRI gantry room.
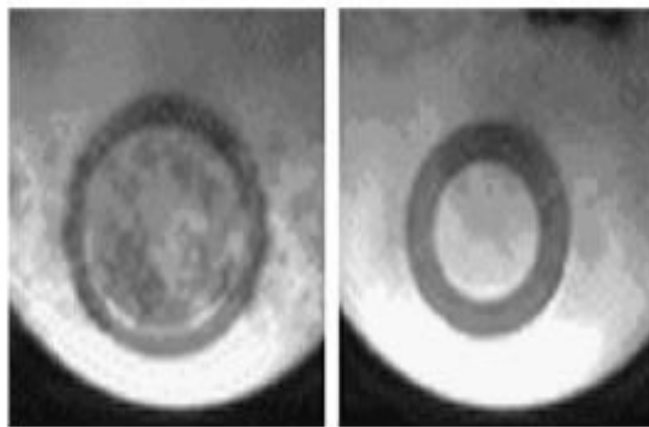
Figure 2.5 MRI cine gradient images of rodent cardiac phantom, diastole phase(left) and systole phase(right) (8)

From the study of heart phantoms described above, two phantoms, Dynamic multi-modal heart phantom or Rodent heart phantom can be used in our study, however, none of above phantoms are for fetal heart. With the work presented here, attempts are made to do ground work for developing a heart phantom for fetus heart and test possibility for rubber balloon as a ventricle instead of materials suggested above. And testing a different driving mechanism. Using suction force for driving balloon opens opportunity for using uni-directional flow valves, which can be considered analogous to Atrio-Ventricular (AV) valve and Aortic or Pulmonary valves.

3   Theoretical Background

This chapter describes physiology of Fetal circulation and fundamentals of MRI and Cardiotocography. Cardiotocography includes various methods of Cardiotography, pattern of signal and feasibility of usage of that method under MRI. Finally we discuss about how a MRI compatible Doppler Ultrasound device is made.

3.1   Fetal Circulation

shows the Diagram of the human feto-placental circulatory system.   A fetal heart functions differently when compared to the newborns or humans, because fetal respiratory system is not in use. During the Gestation period mother provides all the required oxygen and nutrients to the foetus through the Umbilical cord and placenta.
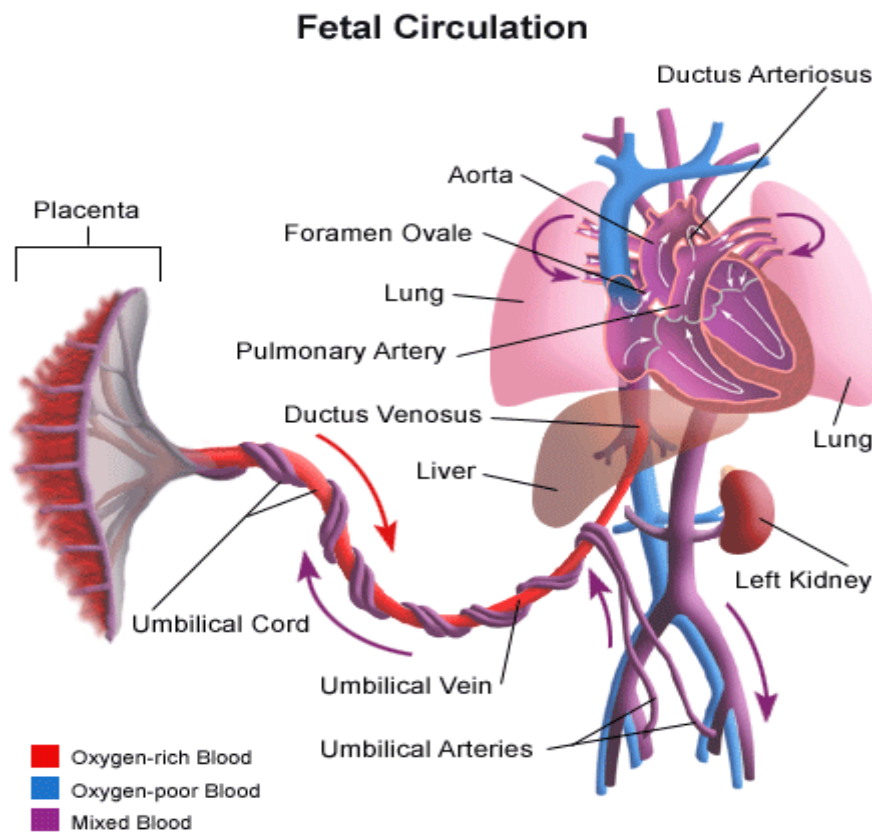
Figure 3.1 Feto-placental circulatory system (24)

Oxygenated blood from the mother first travels through umbilical cord to reach liver and then enters into inferior vena cava. Vena cava leads a path to the right atrium. In the right atrium the blood gets collected first and then passes onto the left atrium. There is an opening between atriums which links left atrium to the right atrium. This opening is known as Foramen-Ovae. Left ventricle gets blood from the left atrium. Left ventricle then pushes

blood through aorta to the fetal circulatory system, supplying blood to the vital organs and muscles. Deoxygenated blood returns to the heart through Superior Vena Cava. Stroke volume.of left ventricle(LV) increases as the foetus develops. Table below shows approximate SV at different gestation period, measured using 2-Dimensinal and Doppler Ultrasonography (25).

Table 3-1 Calculated Stroke volume(approx.) of left ventricle at different gestation period.

Gestation Period	Stroke Volume of LV (ml) measured by 2-D Doppler
20-22 Weeks	0.492
28-32 Weeks	2.310
Intra-Uterine Growth restriction(IUGR) at 26-34 weeks	1.630

3.2 Magnetic Resonance Imaging

Magnetic Resonance Imaging is very useful imaging modality and its usage is rapidly growing because of several advantages. First, It uses strong magnetic field and Rf pulses to gather data for image reconstruction. Usage of magnetic field or Rf pulse has none recorded harmful effects. Second images can be reconstructed at any desired view angle or axis. A brief description about how a MRI system works is given below.

3.2.1 Fundamentals of MRI

Tissue consists of molecules. Molecules consists of elemental atoms. Protons and Neutrons form nuclei of an Atom. These particles gives Nuclear spin to nuclei. Nuclear spin is also known as magnetic moment and it has both magnitude and direction. Under normal conditions i.e. in absence of any external magnetic field magnetic moments of atoms in tissue are randomly aligned and sum of their magnetic moment is almost zero (M=0). When an external magnetic field(B_o) is applied around tissue, a torque acts on nuclei and they tend to get aligned with applied external magnetic field. These alignment can be either parallel(low energy state) or anti-parallel(high energy state) to the applied field. Number of nuclei aligned parallel with external field is little more than the rest, thus giving a net magnetization(Mo) to the tissue.
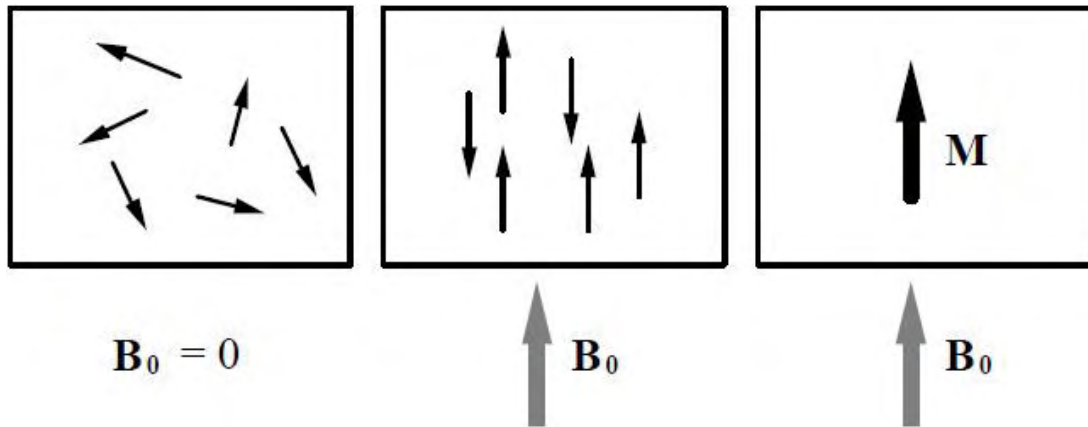
Figure 3.2 First, randomly aligned nuclei in absence of magnetic field. Second, aligned magnetic moment of nuclei in presence of magnetic field. Third, net magnetization(Mo) developed in the direction of applied field (26) (27) .

Magnetic moment of a Nuclei trying to align with external magnetic field shows precession effect. A precession is also known as wobbling effect occurring at a resonant angular frequency. This resonant angular frequency is also known as Larmor frequency. This is given by following equation:

$$\omega_o = \gamma B_o \qquad (3.1)$$

where, ω_o is Larmor frequency, γ is Gyromagnetic ratio,
B_o is Strength of external magnetic field (Tesla)
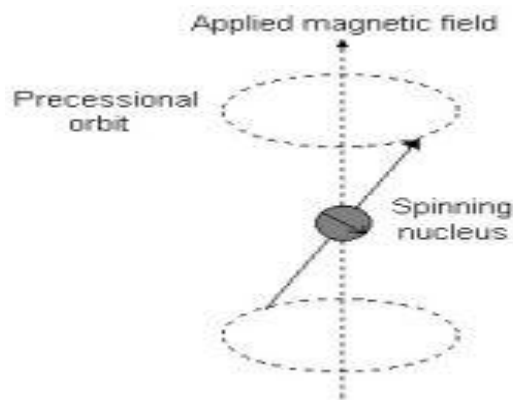
Figure 3.3 Wobbling of nucleus around axis of applied magnetic field at an angular frequency of (ω_o) (27).

Gyromagnetic ratio(γ) varies for atoms of each element. Nuclei aligned in parallel with(B_o) are in low energy state and those aligned in anti-parallel with (B_o) are in higher energy state. Now when sufficient energy is supplied to nuclei, it shifts from lower energy state to higher energy state. The amount of energy required for shifting is given by following equation:

$$Energy\ E = h\omega_o \qquad (3.2)$$

from equation (3.1),

$$E = h.\gamma.B_o \tag{3.3}$$

where, h is $Planck's$ $constant$

The amount of energy required for energy state shifting is dependent on applied external magnetic field strength. This energy is given to the nuclei with the help of Radiofrequency(Rf) pulses. Nuclei absorbs energy supplied and deviates from the external magnetic field direction by an angle (α).

$$\alpha = KT \tag{3.4}$$

where, K is $Constant,$ T is $Pulse$ $duration (Second).$

When magnetic moment of a nuclei absorbs Rf energy and deviates by 90°, the Rf pulse is known as 90° Rf pulse. Similarly for 180° flip. In order to attain lower energy state back, the Nuclei releases absorbed energy exponentially, as shown in Figure 3.4. This process of energy release is known as Free Induction Decay (FID). This exponentially decaying energy is detected using receiver coils around test tissue. The time taken for emission of this energy is known as relaxation time. Two parameters, namely T_1 and T_2 indicate time taken my Mo to return back to its original position. T_1 time corresponds with Mo component along XY plane(Mxy) and T_2 corresponds with Mo component along Z-axis(Mz). This is calculated using following equations:

$$M_z = M_o (1 - e^{\frac{-t}{T_1}}) \tag{3.5}$$

$$M_{xy} = M_o (e^{\frac{-t}{T_2}}) \tag{3.6}$$

These relaxation time parameters vary for different tissues. Based on concentration of certain nuclei in that tissue, information gathered using receiver coil is used to reconstruct images through intense signal processing.
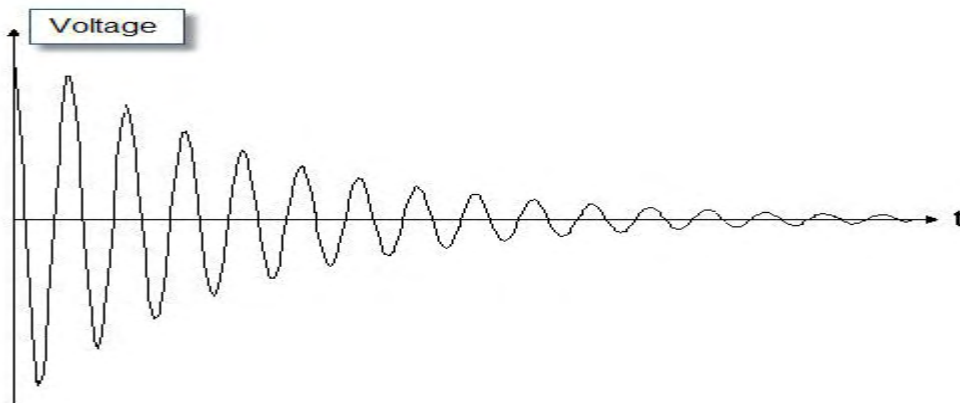
Figure 3.4 Free Induction Decay of Nuclei (27).

3.3 Cardiotocograph

Instantaneous fetal heart rate can be measured and recorded with the help of cardio graphs. There are various clinically accepted methods for monitoring fetal heart. This method causes minimum patient irritation and provides good results. lists various methods employed for fetal monitoring (1):

Table 3-2 Direct and Indirect methods of Cardiotocography.

Indirect (External)	Direct(Internal)
Abdominal fetal electro cardiogram (ECG)	Fetal ECG with scalp electrode
Fetal phonocardiogram	
Ultrasound technique(Doppler)	

3.3.1 Fetal ECG with scalp electrode

This is an example of direct signal recording method. Electrodes are placed in direct contact with the foetus. By this method only fetal ECG signal are obtained, no maternal ECG signal. It's advantage is that signal are of high quality with high signal-to-noise ratio(SNR) as shown in Figure 3.5. Abdominal or Trans-Abdominal electrodes are used when the membrane is not punctured and Scalp electrodes are used after membrane is ruptured. The use method of cardiotocography is limited to delivery period only, hence not a good source of signal for MRI triggering.
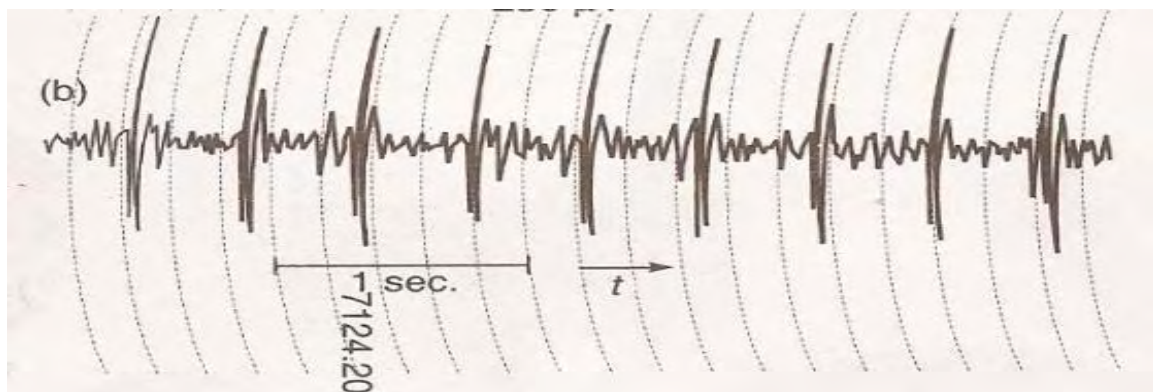
Figure 3.5 Example recording of Fetal ECG using scalp electrode (1). with fileter bandwidth 15-40 Hz

3.3.2 Abdominal Fetal Electrocardiogram(AFECG)

It is an indirect method of recording fetal ECG. Electrodes are placed on maternal abdomen (28) . The resulting signal is a combined signal of maternal ECG signal and fetal ECG signal . Typically maternal ECG signal has an amplitude of about 1mV while fetal ECG signal ranges between 100-300μV. which is about 10-30 times low in amplitude. Also fetal

heart beats at about 120-160 beats per minute (20). This combination of maternal and fetal ECG signal, sometimes, contains additional noise signal as well. Figure 3.6 shows an example recording of fetal electrocardiogram (1). This noise signal is generated by number of reasons. Few common noise sources are muscle noise, polarization of electrodes. This makes it really difficult to measure and record Fetal ECG. Properly designed signal processing technique can help in suppressing noise. Signal Averaging (1) (29) (30) is one of many popular technique used for signal processing. This technique is useful for ECG recording under normal conditions. While under MRI, strong magnetic field and Rf signal adds additional electrical noise into the ECG signal, making it even more difficult to process and gather reliable fetal ECG signal data. Therefore this method is least suitable as source of signal for MRI triggering.
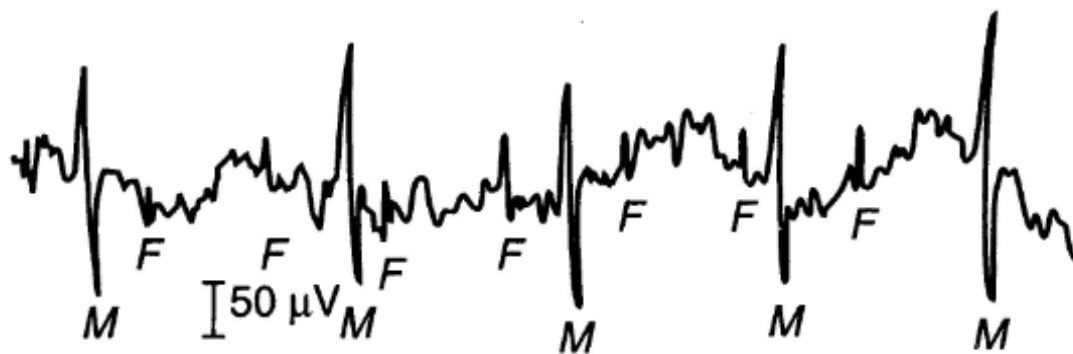
Figure 3.6 Example recording of fetal electrocardiogram with filter bandwidth of 0.2-200Hz (1)

3.3.3 Fetal Phonocardiogram

A sensitive microphone is placed over maternal abdomen and fetal heart sounds are recorded. Normally two heart sounds, relating to contraction and relaxation of the heart muscle are easy to detect and record. This technique has an advantage that it can provide better baseline FHR data compared to Ultrasound, considering ideal conditions, noise less environment , advance signal processing. The disadvantage of this technique is that microphone picks up a lot of ambient noise including uterine contractions, maternal movements. Also, sometimes, the depth of foetus affects in signal recording. While MRI starts data acquisition it makes a lot of noise. Because of high sensitivity of microphone to pick up surrounding noise along with fetal heart sounds its less suited for our purpose. Even in daily use this method is less preferred because of its this disadvantage. Figure 3.7 is an example of such phonocardiogram signal along with murmurs (31).
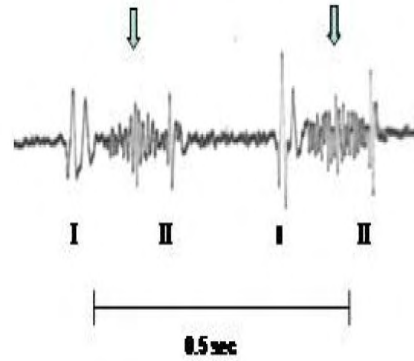
Figure 3.7 Presence of murmurs in Phonocardiogram, indicated by arrow (31). Image is a photograph taken of a signal displayed on an oscilloscope.

3.3.4 Ultrasound Doppler Technique

This method works on the principle of Doppler shift. According to Doppler shift law a change in frequency occurs when a body moves with respect to the observer. When the body moves towards the observer the frequency shifts to higher wavelength. This is also known as Blue shift. And when the body moves away it shifts toward lower wavelength. This is known as red shift. This frequency shift can be calculated according to following equation:

$$\Delta f = (2 \cdot f_o \cdot u \cdot cos\theta)/c \qquad (3.7)$$

where, Δf is the magnitude of frequency shift, f_o is the transmitted frequency, u is the velocity of moving body, c is the velocity of sound wave in the tissue, $cos\theta$ is the cosine of the angle of the sound beam.

Normally, fetal heart lies about 5-20 cm under abdomen, depending upon probe position and fetal orientation. For studying fetus Ultrasound frequency between 2-2.5 MHz is used (1). Following is a general block diagram of a Doppler device (1):
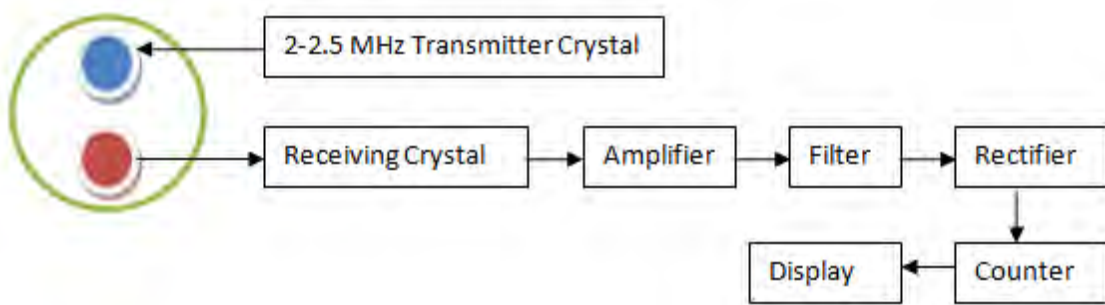
Figure 3.8 General Block Diagram of a Doppler Ultrasound device.

Figure 3.9 Single element hand-held portable Doppler device (32).

Depending upon the number of crystal used and type of arrangement a Doppler Cardiotocograph can be classified into either narrow beam or wide-angle beam device. A narrow beam device uses only a single pair of transmitter/receiver crystal. For e.g. hand held device shown in Figure 3.9. In a wide angle beam device more than one transmitter receiver pair is used. For e.g. transducer probe shown in Figure 3.10 (6). Use of many receiver crystal helps in covering signal coming from wide area, thus helping in quick detection of heart movement.
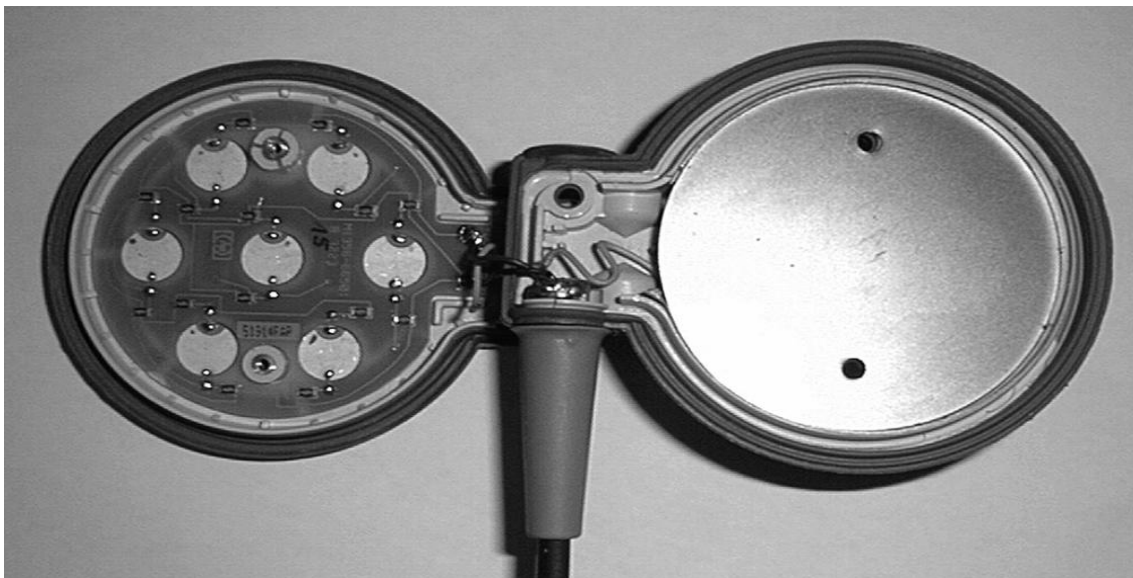
Figure 3.10 Transducer with multiple receivers (6). Multi-element transducer helps in covering larger area for signal detection. The transducer is modified for use in MRI.

Research works can be found in favour of Doppler device usage under 1.5T MRI system (6). Use of an electronic probe under MRI carries a lot of noise induced by Rf signal

of the MRI system. To solve this problem, a fetal monitor was modified by removing ferro-magnetic materials from the probe and shielded by using Titanium plates (6). Copper wires should be properly shielded and connected to MRI system's ground. In our development process we use modified Hp 8040A fetal monitor.

4 Design principle, Materials and Construction

4.1 Concept

By studying design of phantoms discussed in chapter 1 and from observations from the lab experiments it was clear that a simple rubber water balloon can be inflated and deflated with water to get sufficient Doppler shift. Also a remotely operated driving mechanism is used to pump water/fluid inside balloon and out of balloon periodically. In our design we create suction force inside balloon to force water/fluid to flow inside it and use balloons elasticity to push water/fluid outside. Use of uni-directional flow valves can help in limiting the flow of fluid in one direction.

4.2 Block Diagram

Figure 4.1 shows block diagram for the Heart phantom design.
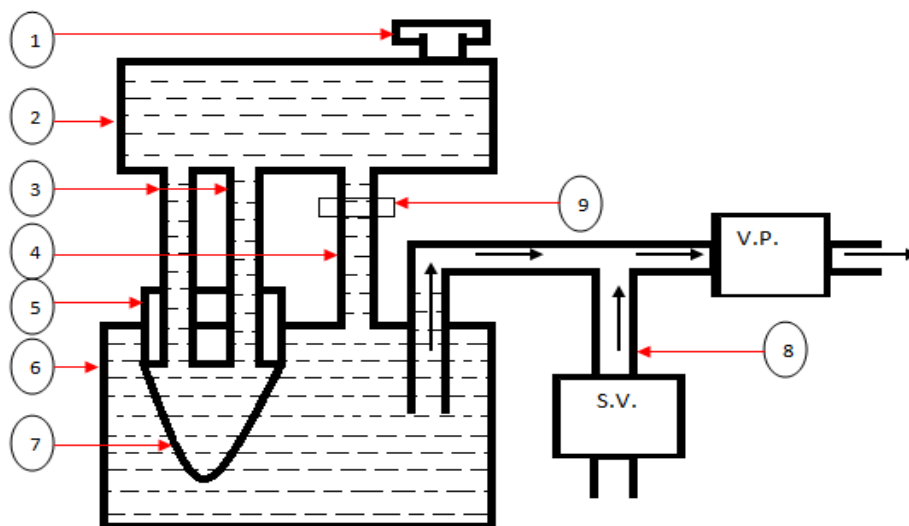
Figure 4.1 Block Diagram of the phantom. This design uses no uni-directional valve and uses a closed fluid reservoir for flow of fluid.

In Figure 4.1:

1. Opening for water filling.
2. Acrylic chamber filled with water.
3. Silicone hose connecting Balloon with above acrylic chamber (2) filled with water.
4. Silicone hose connecting Below water filled acrylic chamber (5) with above acrylic chamber (2) filled with water.
5. Balloon holder fitted over second chamber. This helps in fitting a balloon as well as connecting two silicone tubes.
6. Second Acrylic chamber, holds balloon inside.
7. Balloon

8. Silicone hose connecting second water filled chamber to a vacuum pump and a solenoid valve.
9. Clip for blocking link between two acrylic chambers.

Solenoid Valve(S.V.)

Vacuum Pump(V.P.)

Description:

A Doppler device detects moving body and accordingly detects frequency shift in the ultrasound signal. In this design the Balloon acts as moving body. Both acrylic chambers, balloon and connecting hose, accept the one connecting to vacuum pump and a solenoid valve, are filled with water. Once the water is filled the opening for water filling is closed. The silicone hose connecting the two acrylic chambers is also blocked. When vacuum pump is turned on the air filled in the connecting hose is sucked out in to the atmosphere. The vacuum thus created makes water to rise into the hose and creating a vacuum in the connected acrylic chamber. The water from the first chamber flows in the second chamber to fill up the vacuum thus forcing balloon to inflate. This action is analogous to systole phase of a heart ventricle. When an electric pulse is applied to the ventricle muscle, the muscles expand causing ventricle to inflate and creating a negative pressure in them. This negative pressure forces the Atrio-ventricular(AV) valve to open and allows blood to flow in. Now when the vacuum pump is turned off and a solenoid valve is opened the elasticity of the balloon tries to resume its neutral position because the vacuum in the hose is filled air. The air comes in through the solenoid valve. This elasticity of the balloon and the vacuum created in the first chamber because of inflow of water is the driving force for water to return back in to the first chamber. This action is analogous to diastole phase of the heart ventricle. When this process of opening and closing of Solenoid valve is controlled properly and repeated the ventricular action of a heart can be reproduced. Inflation and deflation of the balloon helps in producing the Doppler signal for the CTG. The frequency of the signal provided to the solenoid valve is reflected on the Doppler device as beat per minutes.

Another design was proposed with a slight change in above design as shown in Figure 4.2. In this design first chamber, silicone hose(connecting balloon, second chamber with the first chamber) were replaced by uni-directional mini valves. And the setup was placed in a vessel filled with water. The driving mechanism remained same as to be used with above design. Pictures of this second design, valves used is described in Appendix I. While testing this phantom under 1.5T Philips Achieva system it was observed that the air pocket between water level and imaging coil creates artifacts in the reconstructed images. Also when then

phantom was placed in a closed vessel it affected its performance and temporary deformation in valves. Because of all this reasons, further development in this design was discontinued.
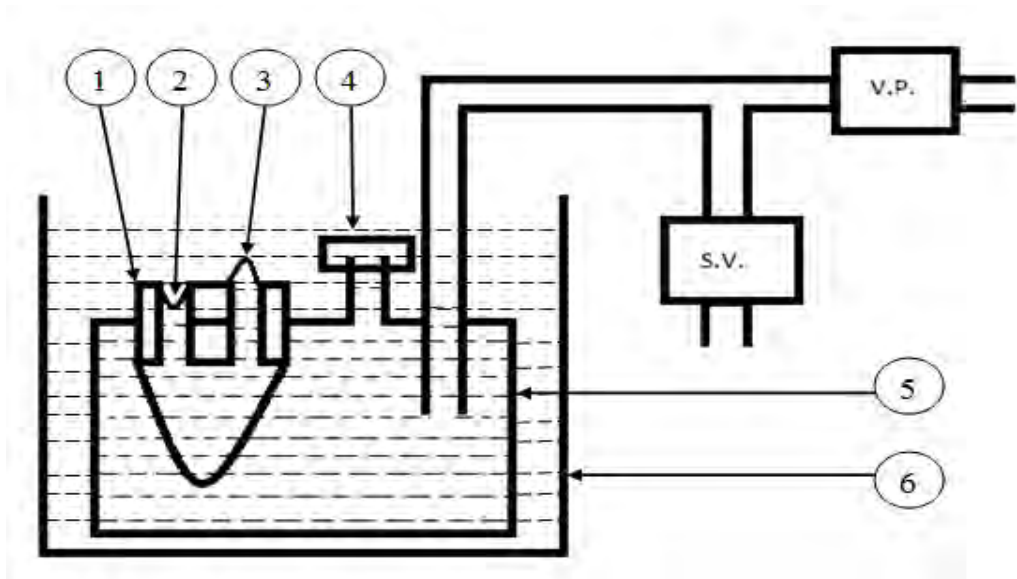
Figure 4.2 Block diagram of the second design, including unidirectional valves.

In Figure 4.2

1. Balloon-valves holder
2. Inlet unidirectional valve
3. Outlet unidirectional valve
4. Opening for filling water in the chamber
5. Inner vessel filled with water and containing balloon and valves
6. Out vessel filled with water

Solenoid Valve(S.V)

Vacuum Pump(V.P)

4.3 Construction

From the description of design it is clear that the phantom has three important parts. Each part has to be constructed separately with special materials and then put together. These three parts of the phantom are:

1) Reservoir chamber
2) Ventricle chamber
3) Control box.

4.3.1 Reservoir chamber

This first chamber acts as a reservoir chamber. From here the water flows to balloon in the second chamber and vice versa. The tap on the top helps in filling the whole setup with

water and also closed it helps in creating vacuum, so that water in balloon is forced to return back. The material chosen for this chamber is a <u>Acrylic pipe</u>. A piece of acrylic pipe is covered with the help of covers made from PVC (Poly Vinyl Carbonate). Covers are glued with the acrylic pipe using thick acrylic glue and silicone glue. This material has more strength, transparent and is MRI compatible. Figure 4.3 is the picture of the first chamber. Two out of three bottom opening are connected to the balloon holder, placed in second chamber. Silicone tubes of inner diameter of Ø8mm were used for connection. Projection drawing and dimensions can be found in Appendix III(a, b).

Figure 4.3 Reservoir chamber filled water, It has a top opening and three bottom opening for connection with ventricular chamber using silicone pipes.

In Figure 4.3

1. Bottom PVC cover
2. Plastic clip for blocking pipe connecting First chamber to the second chamber. When this clip is opened, it helps in filling second chamber with water.
3. The connecters at the bottom of the first chamber. Two connecting with balloon and one for second chamber.
4. Top PVC cover
5. Opening for filling water in the system.

4.3.2 Ventricle Chamber

The second chamber holding rubber water balloon is called as a ventricle chamber because we assume balloon as a ventricle of heart. The second chamber is the main focus area of imaging under MRI. Figure 4.4 shows the second chamber designed for phantom. As shown it has to accommodate a balloon which will act as a ventricle. One opening will

connect it to the first chamber and second will link it to the Vacuum pump and a Solenoid Valve. The material chosen is Acrylic pipe. The top and the bottom covers are made from PVC (Poly Vinyl Carbonate) Plastic. A Balloon holder is designed for holding balloon. Projection drawing and dimensions can be found in Appendix III(a, b, c, d).
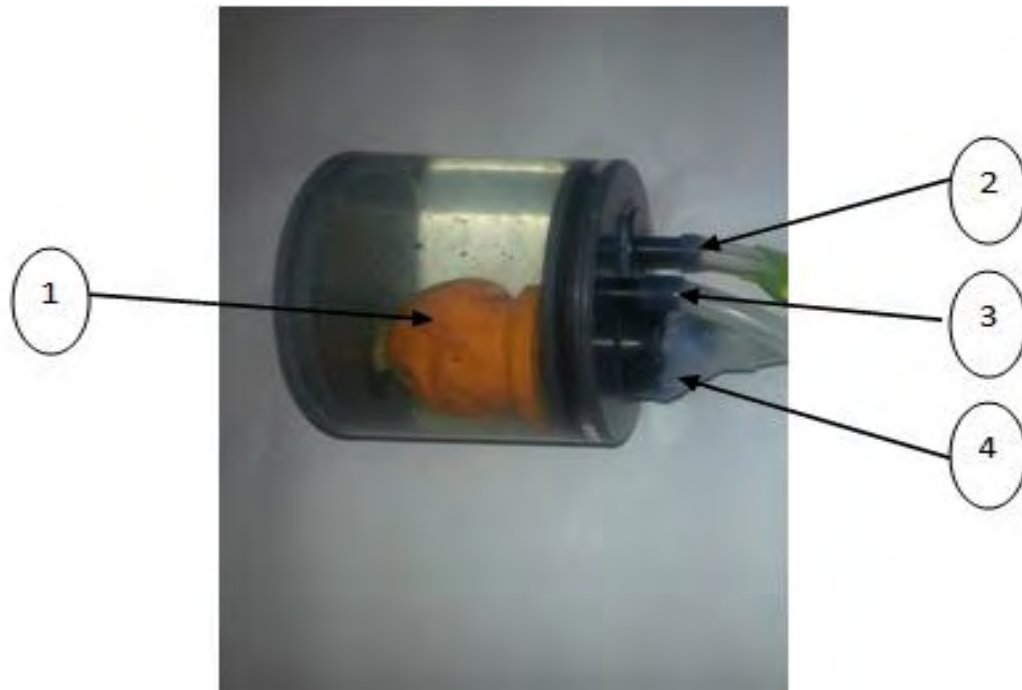
Figure 4.4 Second chamber as a ventricle chamber. A water balloon is cut and fixed with balloon holder. Bottom is glued at the bottom to give it a ventricular like shape.

In Figure 4.4

1. Water Balloon (Orange)
2. Connection for First chamber
3. Connection for Control box
4. Balloon holder

4.3.2.1 Top Cover

Figure 4.5 is shows top cover. It is made out of PVC material. A holder for balloon is fitted on it. 2D projection drawing is attached in Appendix III. Black colour O-ring holds it tight with the acrylic tube.

Figure 4.5 Top cover for second chamber

4.3.2.2 Top cover for Ventricular Chamber

Figure 4.6 shows balloon holder. There are two threaded regions. Bigger thread region fits with the top cover as shown in Figure 4.7. A water balloon is fitted over periphery of the nut which fits over second, small, threads on the holder. After that It is covered with Silicone gel to prevent any leakage. Water balloon's apex is stick with the bottom layer of the chamber with the help of two component glue. By doing so air bubbles can be removed which seldom get trapped inside. Two holes of Ø12mm serves two purposes. In one design two unidirectional valves are fitted on it as shown in Figure 4.8. And In second design it is used to connect two silicone pipes which connects with first chamber on other end as shown in Figure 4.9.

Figure 4.6 Balloon holder with two Ø12mm holes for holding valves or connecting silicone pipes.

Figure 4.7 Balloon holder fitted on top cover

Figure 4.8 Holder with two uni-directional valves facing opposite direction

Figure 4.9 Holder with two Ø8mm silicone tubes fitted and covered with silicone glue.

4.3.3 Control Box

A Control box is necessary for controlling amount of systolic-diastolic action of the balloon and also its repetition rate. As shown in block diagram, Figure 4.1 and Figure 4.2, a vacuum pump sucks out air from the connected hose. Because of this suction a vacuum is created and cause water in the pipe to rise up and balloon to blow out. The void is filled with the water from first chamber. This vacuum is released when the solenoid valve is opened. By opening solenoid valve we allow air to rush into the pipe. Thus giving an opportunity to the balloon to relax. For simplicity a vacuum pump is running continuously and solenoid is

turned ON/OFF periodically. Duration of On/Off is controlled with the help of Pulse width modulation.

Figure 4.10 view of the control box. 6 Rocker switch for controlling V.P. and S.V.. Two potentiometers for pulse width and Front frequency control.

Figure 4.10 shows front view of the control box. In front there are six switches. Start from left, first switch is an ON/OFF switch for power supply used for Vacuum pumps. Next four switches are for each vacuum pump. And the most right switch is for Solenoid valve.
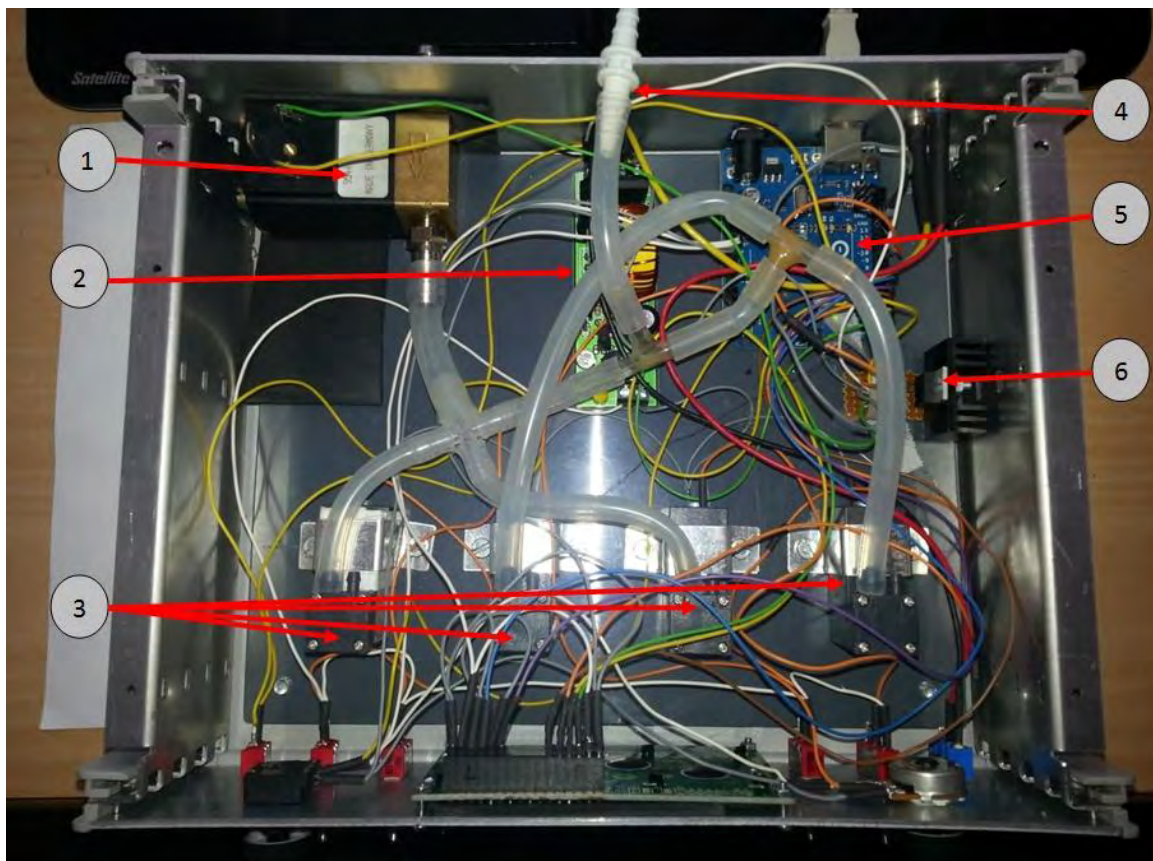
Figure 4.11 Setup of components inside control box.

Figure 4.11 shows internal setup for the control box. In this picture, (1) is Solenoid Valve, (2) is step down power voltage regulator for vacuum pumps, (3) four vacuum pumps

used, (4) point of connection for Silicone pipe coming from phantom, (5) is an Arduino UNO board for pulse generation, (6) is MOSFET for connecting solenoid coil. Description connection and working is given below.

4.3.3.1 Control of Vacuum pump

Vacuum pump used in control box is mini vacuum pump which runs on dc power. Figure 4.12 shows vacuum pump used (33). It's a 2L/min mini vacuum pump operating with 12V DC power supply.

Figure 4.12 A mini Vacuum pump with 2L/min flow.

A heart phantom should be operable between 60-160 beats per minute range. Assuming 130 as maximum beats per second value we get only

$$\frac{60}{130} = 0.4615 \ sec$$

for each cycle. In this 0.461s time sufficient vacuum must be created and also give enough time for air to fill up that vacuum. Now a single vacuum pump operating at 12V displaces 2L air per minute. So it displaces about

$$\frac{2000 \ ml}{60 \ sec} = 33.33 ml$$

of air per second. And assuming that solenoid valve is operated with 50% duty cycle pulses

$$\frac{0.4615}{2} = 0.2307 sec$$

the vacuum pump will displace approximately

$$0.2307*33.33= 7.6908 \ ml$$

of air in one cycle. The silicone pipe connecting phantom with V.p. is very long and hence the displacement of only 7.6908ml of air is very less. This small amount of air displacement will not generate enough suction force on balloon to inflate. Or the movement will be negligible. Therefore multiple vacuum pumps were used, operating in parallel to create enough displacement of air in short amount of time. Instead of that one big pump could have also been used. But when operating at low beats per second setting this displacement becomes huge and give balloons tends to burst. This could be controlled by varying supply voltage to the pump but controlling vacuum pump supply voltage is also a challenging task. By using multiple small pumps in parallel a similar control could be obtained by simply connecting a switch. Thereby operating only a pump when needed and as per requirement. Figure 4.13 shows circuit diagram for connecting vacuum pumps with a regulated power supply. A 22V/2A variable power supply is used for supply power to vacuum pumps (34).
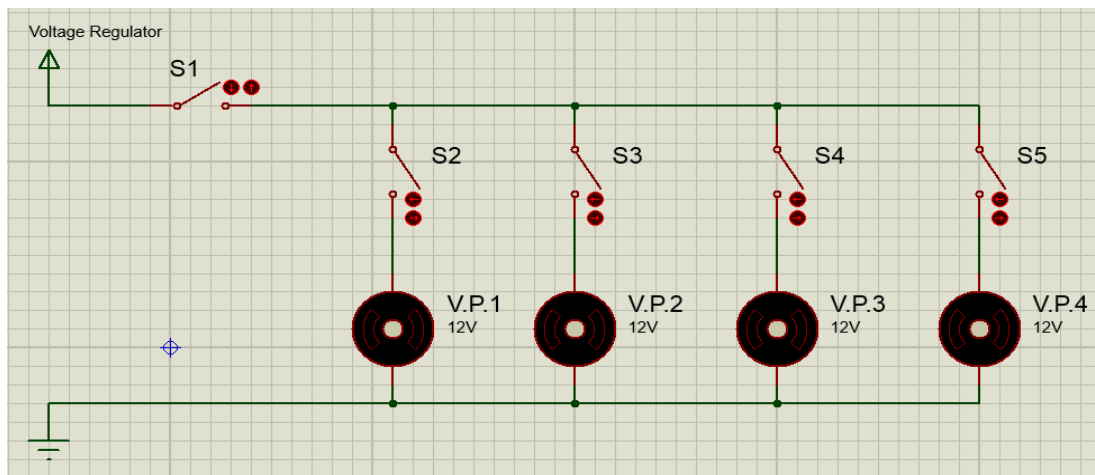
Figure 4.13 Circuit diagram for Vacuum pump connection. Switch S1 is the main control. Switch S2-S5 help in controlling number of operating V.P.

4.3.3.2   *Control of Solenoid Valve*

A Solenoid valve is an Electromechanical device (35). A plunger is connected to an electric coil. It is used to open/stop flow of air into the system to fill the vacuum created by Vacuum pump. When an electric current is applied to this coil the plunger moves and thus either opening or closing the valve. In our case when an electric current is applied to the coil, the plunger opens and allows the Air to flow into the system. And when the coil is de-energized i.e. no current applied, the valve is closed. Thus air flow stops and Vacuum pumps gets a chance to create a vacuum in the system. A 24V 1/4" solenoid valve is used for our use. A control mechanism for controlling Open/closing of the Solenoid valve is very important, as the cycle of opening/closing of the valve is reflected on balloon's action. A control circuit is designed to generate clock pulse of appropriate frequency and variable

pulse width so that the electric coil in the valve can be energized properly. For ease of development an open source electronic development tool known as <u>Arduino</u> <u>UNO</u> is used, shown in Figure 4.14. Arduino is an open-source development tool for developing hardware-software according to specific needs. User friendly development environment is available for programming onboard microcontroller. A guide on using Arduino development environment is available on Arduino website <u>http://arduino.cc/en/Guide/Environment</u>. With the help of Arduino we generate pulses for the Solenoid valve of appropriate frequency and pulse width with the help of two control potentiometers. One is used for setting necessary frequency and second for controlling pulse width. By controlling pulse width we can control the close time of the solenoid valve thereby controlling amount of systolic movement of the balloon.
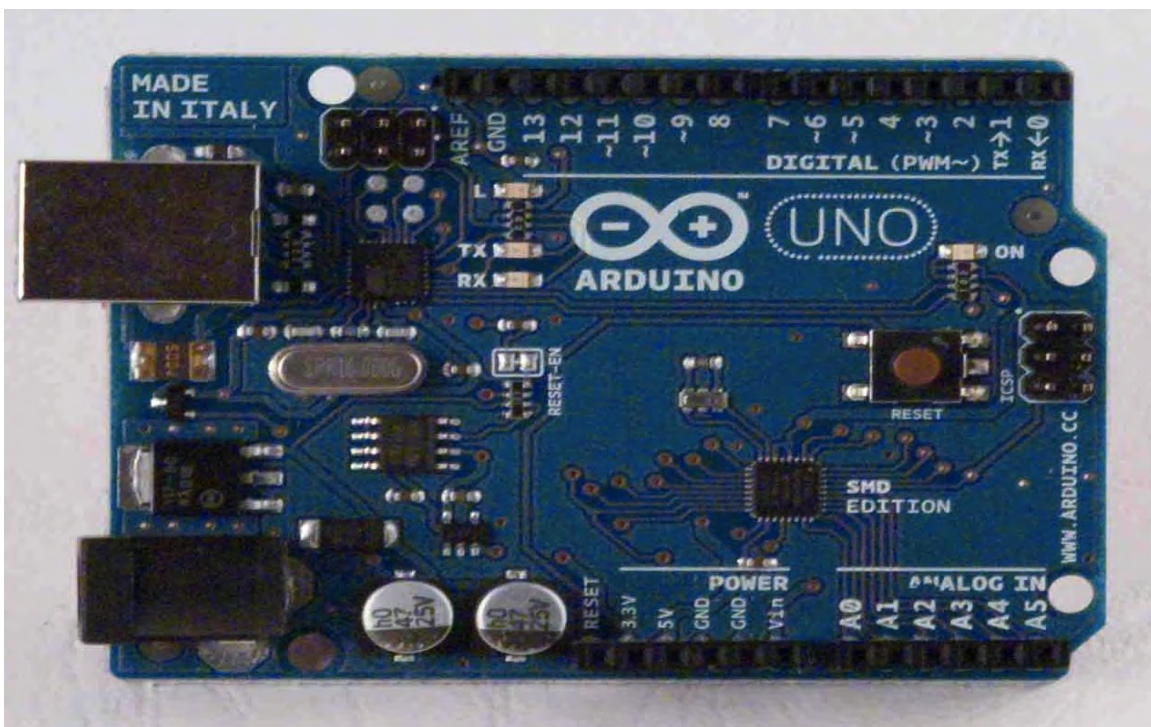
Figure 4.14 Arduino UNO development board with Atmega328P microcontroller.

For e.g. If we are generating 60 pulse per minute and we have a pulse width of 30% while the vacuum pump is working continuously. The balloon will inflate to a certain amount, say X. Now if we change the pulse with to 60% the balloon will inflate, approximately, half the amount then before(X/2). By allowing the valve to remain open for longer timer we let more air to pass in there by matching the amount of air sucked out by vacuum pump and the amount of air flowing in through Solenoid valve. By controlling the number of vacuum pumps operating at a particular frequency and pulse width of pulse supplied to Solenoid.

Table 4-1 Specification of Arduino UNO development board.

Parameter	Value
Microcontroller	ATmega328
Operating Voltage	5V
Input Voltage(recommended)	7-12V
Digital I/O Pins	14(6 for PWM)
Analog Input Pins	6
Clock speed	16 MHz

Out of 14 Digital I/O pins 6 pin(pin number 0-5)are for LCD Display, on which the set heart rate and PWM value is displayed. Pin 9 is used as pulse signal output. Figure 4.15 shows configuration for LCD drive, control pot and pin out for driving coil of a solenoid valve. Two potentiometers of value 10K are used for adjusting PWM and BPM values. Figure 4.16 shows connection for pin 9 to MOSFET. A software was written in embedded C language for continuously scanning the value of both potentiometers and calcuationg and adjusting width of pulse signal and loaded in on-board atmel microcontroller ATMega328P memory. A copy of this code is attached in *Appendix IV*.   Arduino UNO development board offers 6 PWM pin acting in pairs (36). Each pair linked with each timer on chip. Table 4-2 Timer to pin connection and size. shows link of each pin pair with respective Timer and its size.
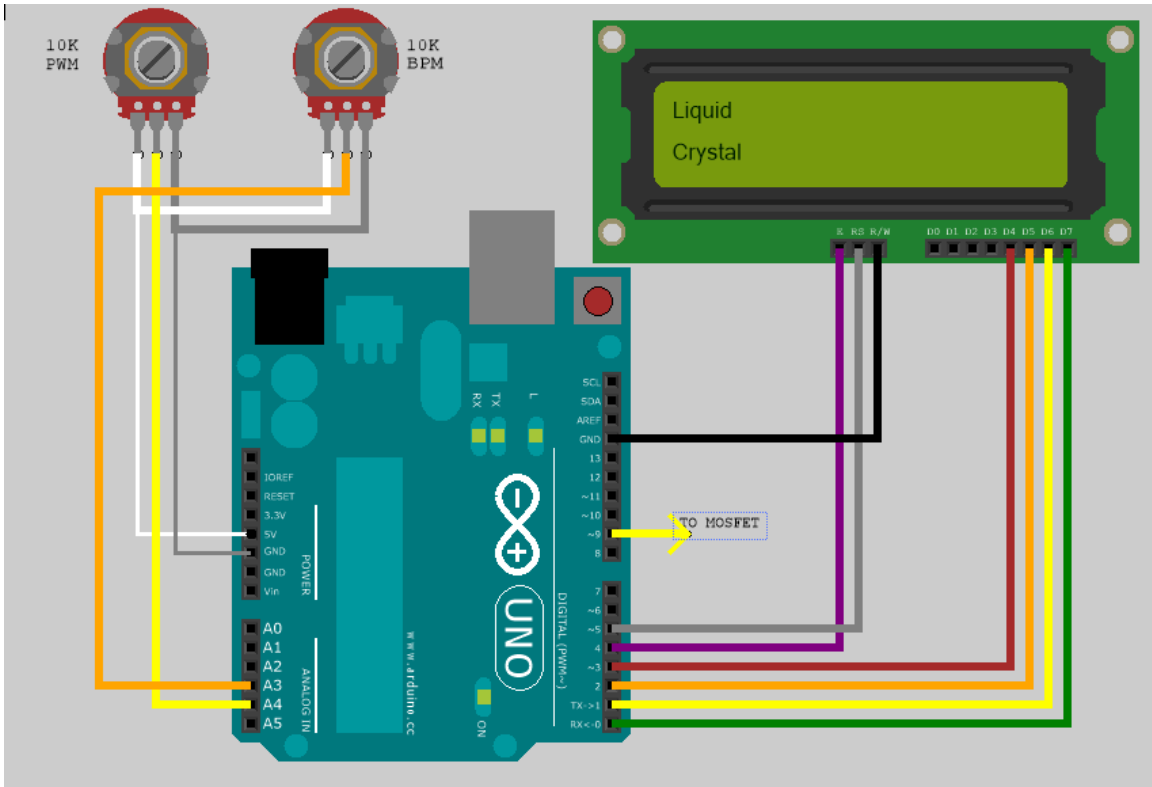
Figure 4.15 Connection diagram for Arduino UNO, 2 POTS, LCD and pin out for MOSFET.
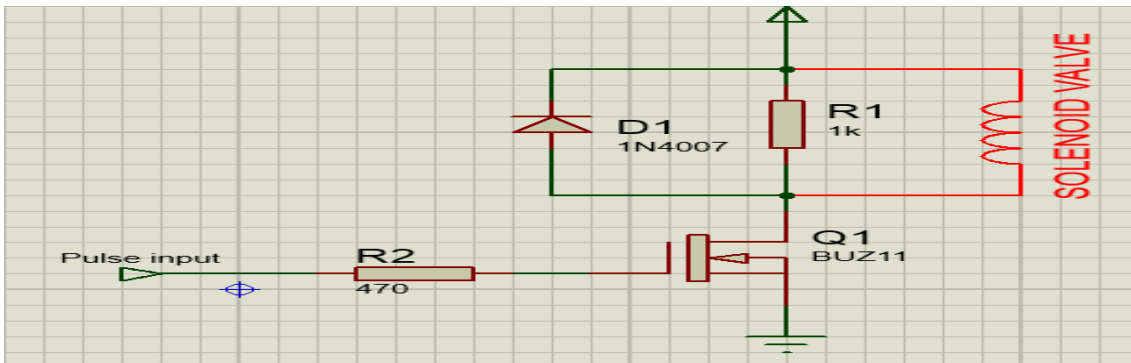
Figure 4.16 Circuit diagram for driving Solenoid valve.

Table 4-2 Timer to pin connection and size.

Timer0	Pin 5-6	8-bit
Timer1	Pin 9-10	16-bit
Timer2	Pin 11-3	8-bit

Compare to 8-bit Timer 16 bit Timer allows more accurate control over wave generation. Each timer has respective set of registers which for respective count number. These registers are Timer/Counter(TCNT), Output Compare Registers(OCR A/B), Input Capture Register(ICR). More details about timers and respective timers can be found in the datasheet of ATmega328P microcontroller. Since we are using a 16-bit Timer for wave generation we concentrate our calculation and development to respective registers and pins.

Timer1 is linked with pin 9-10 on the board. Now Input Capture register holds value according to which output frequency is calculated. Input Capture Register is a 16-bit register. So It can hold value between 0-65535. Output frequency can be calculated according to following formula.

$$Output\ frequency = \frac{f}{2*N*V} \tag{4.1}$$

Here, f is main clock frequency, N is pre $-$ scalar, V is $ICR1$ value.

Atmega328P on Arduino board is operated at 16MHz frequency. Therefore, $f = 16MHz$. Value of Pre-scalar is set according to configuration of Clock select bits. Table 4-3 helps in understanding this configuration, according to Atmega328P datasheet.

Table 4-3 Clock select bit description.

CS12	CS11	CS10	Description
0	0	0	No clock source (Timer/Counter stopped).
0	0	1	clk$_{I/O}$/1 (No prescaling)
0	1	0	clk$_{I/O}$/8 (From prescaler)
0	1	1	clk$_{I/O}$/64 (From prescaler)
1	0	0	clk$_{I/O}$/256 (From prescaler)
1	0	1	clk$_{I/O}$/1024 (From prescaler)
1	1	0	External clock source on T1 pin. Clock on falling edge.
1	1	1	External clock source on T1 pin. Clock on rising edge.

Higher value of Pre-scalar value helps in achieving lower frequency wave signals. As 1024 is the maximum possible pre-scalar value possible, we will use that value. Therefore we choose, $N = 1024$. Now, we calculate the value of ICR1 for desired frequency wave signal. Suppose we want to have BPM of 72. This means 72 beats per minute. Therefore we desire an output frequency of

$$Output\ frequency = \frac{72\ beats}{60\ sec}$$

$$\therefore Output\ frequency = 1.2\ Hz$$

Now, To calculate the value of ICR1 register:

$$V = \frac{f}{2*output\ frequency*N} \tag{4.2}$$

$$\therefore V = \frac{16MHz}{2*1.2*1024}$$

$$\therefore V = 6510.4166$$

For simplicity we round 6510.4166 value to round it to 6500. Table below shows calculated values for different frequency signal generation. Performance of these values were

tested with the help of a portable Doppler device to see if it's able to show same BPM value as set by this control box. And the results were satisfactory with an error of ±2 BPM displayed on indicator.

Table 4-4 Calculated and actual values set in for ICR1

BPM	Output frequency	Calculated V Value	ICR1 value(approx. rounded)
39	0.6500	12019.2308	12000
40	0.6667	11718.7500	11500
42	0.7000	11160.7143	11000
44	0.7333	10653.4091	10500
46	0.7667	10190.2174	10000
49	0.8167	9566.3265	9500
52	0.8667	9014.4231	9000
55	0.9167	8522.7273	8500
59	0.9833	7944.9153	8000
62	1.0333	7560.4839	7500
67	1.1167	6996.2687	7000
72	1.2000	6510.4167	6500
78	1.3000	6009.6154	6000
85	1.4167	5514.7059	5500
93	1.5500	5040.3226	5000
104	1.7333	4507.2115	4500
117	1.9500	4006.4103	4000
133	2.2167	3524.4361	3500
156	2.6000	3004.8077	3000
187	3.1167	2506.6845	2500

After constructing each part of the phantom they are connected together using silicone pipes as shown in Figure 4.17The phantom is filled with water. The phantom is placed in the MRI gantry in horizontal position. A silicone pipe is connects second chamber with the control box, which is placed outside MRI gantry room. Control box controls operation of the phantom for different BPM settings. Cross sectional images(short axis) are obtained to study movement of balloon(ventricle) during systolic and diastolic phase of rhythm.
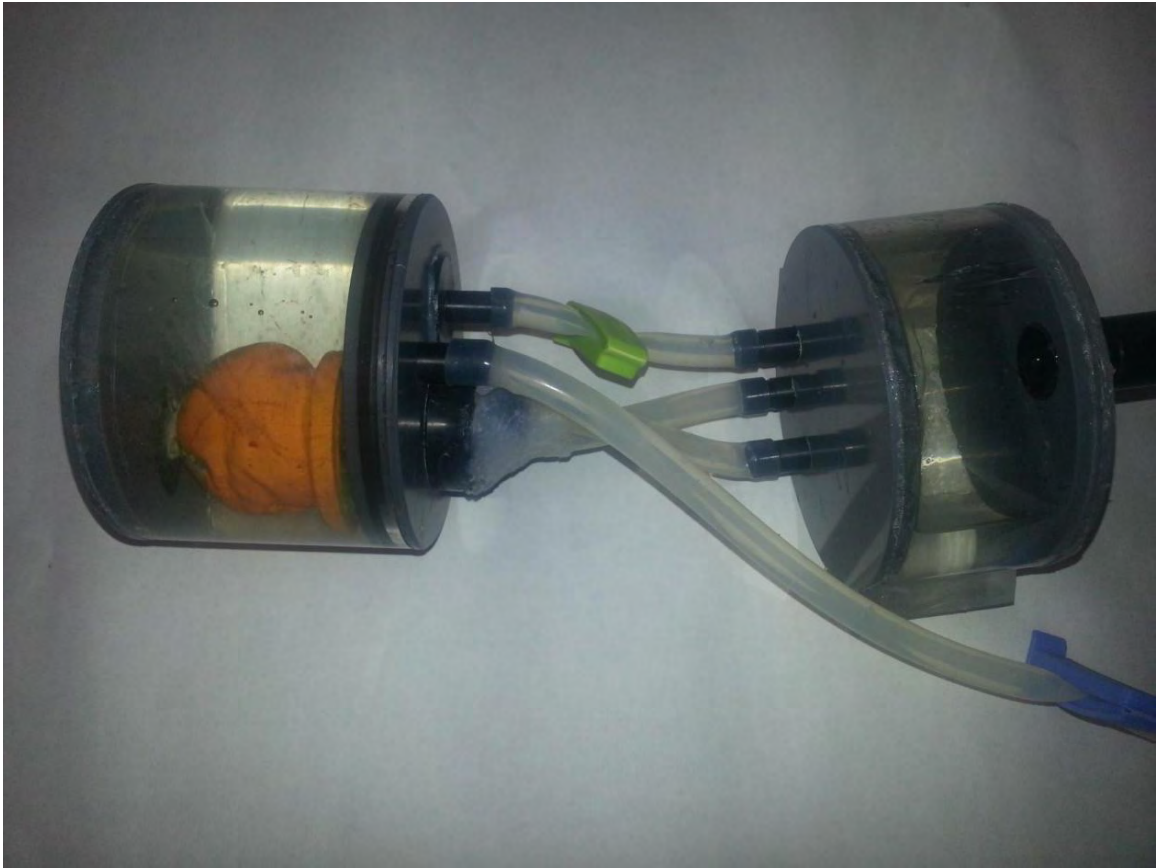
Figure 4.17 Reservoir chamber and Ventricle chamber are connected together using silicone pipes, another silicone pipe connects both chamber and is blocked using a plastic clip(green). A silicone pipe(blocked by purple clip) connects it with control box operating outside MRI gantry room.

5 Phantom test with MR

5.1 Method

The phantom was tested under 1.5T Philips Achieva MRI system for different settings. Figure 5.1 shows block diagram of the setup used for testing phantom with MRI. Three different settings were used to test the phantom. Settings set on control box during the test are listed in Table 5-1. Test was repeated for 93 bpm settings again for confirmation of results.

As shown in figure Figure 5.1 Doppler device's probe was placed on wall of phantom wall, using ultrasound gel in between for impedance matching. The signal was processed by the device and integrated signal was sent to the computer where local peaks were detected and trigger signal was given to MRI work station.
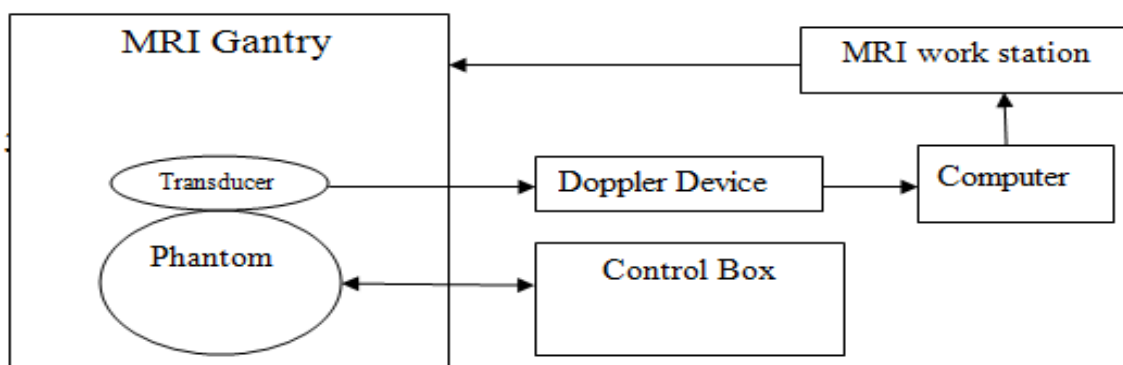
Figure 5.1 Setup for testing Phantom with MRI.

Table 5-1 Settings for Control Box during MRI tests.

Test	BPM	Duty cycle(%)	V.P. (ON)
	62	37.5	2
Test1	93	42.1	3
	133	42.1	3
Test 2	93	42.1	3

Cine gradient-echo sequences were obtained for each setting set the phantom. Parameters set for data acquisition are listed in Table 5-2. A set of frames for each slice were obtained and processed for further calculations.

Parameter	Test1	Test2
Echo time	1.467	1.348
Flip angle	60°	60°
Image matrix	256*256	256*256
Slice thickness	7mm	10mm
Interval between slice	7mm	10mm
Number of frames per slice	30	30

5.2 Results

5.2.1 Plot of Doppler and Trigger signal

Main purpose of having a phantom was to get good Doppler signal so that MRI can be triggered properly and regularly. To test this Doppler signal were acquired by the fetal doppler device and sent to computer after initial signal processing. Local peaks in doppler signal were detected and MRI was triggered.
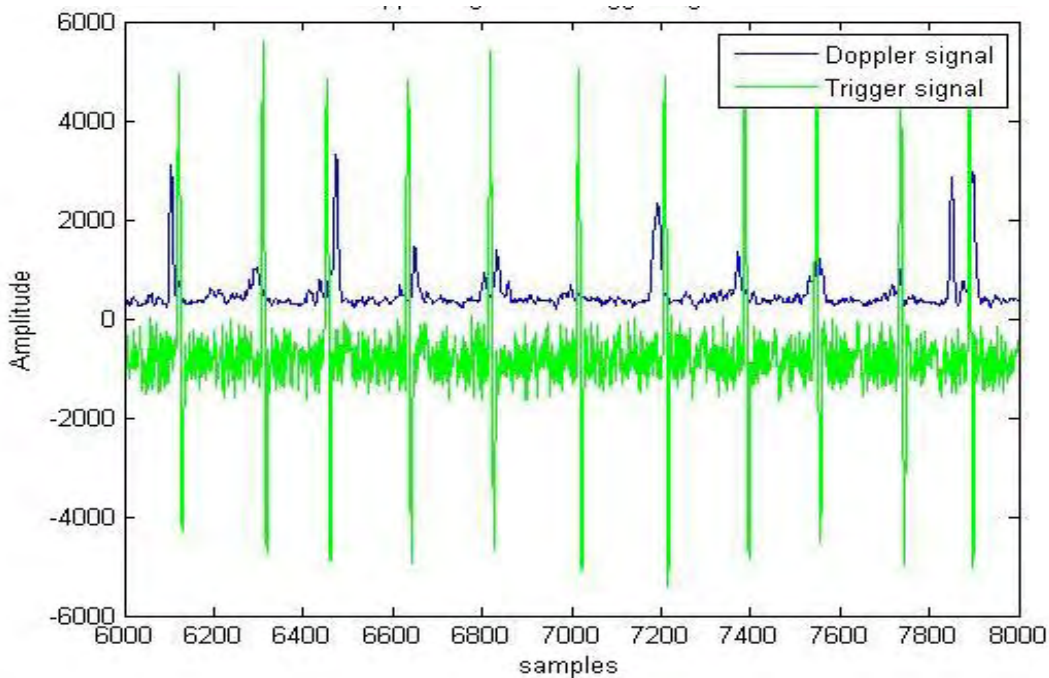
Figure 5.2 Location of trigger signal with respect to Doppler signal for phantom operating at 63 bpm.

Figure 5.2 and Figure 5.3shows plot of rectified doppler signal and location of trigger signal. Triggering was periodic and didn't miss a beat but the position of trigger pulses varied depending on signal quality.
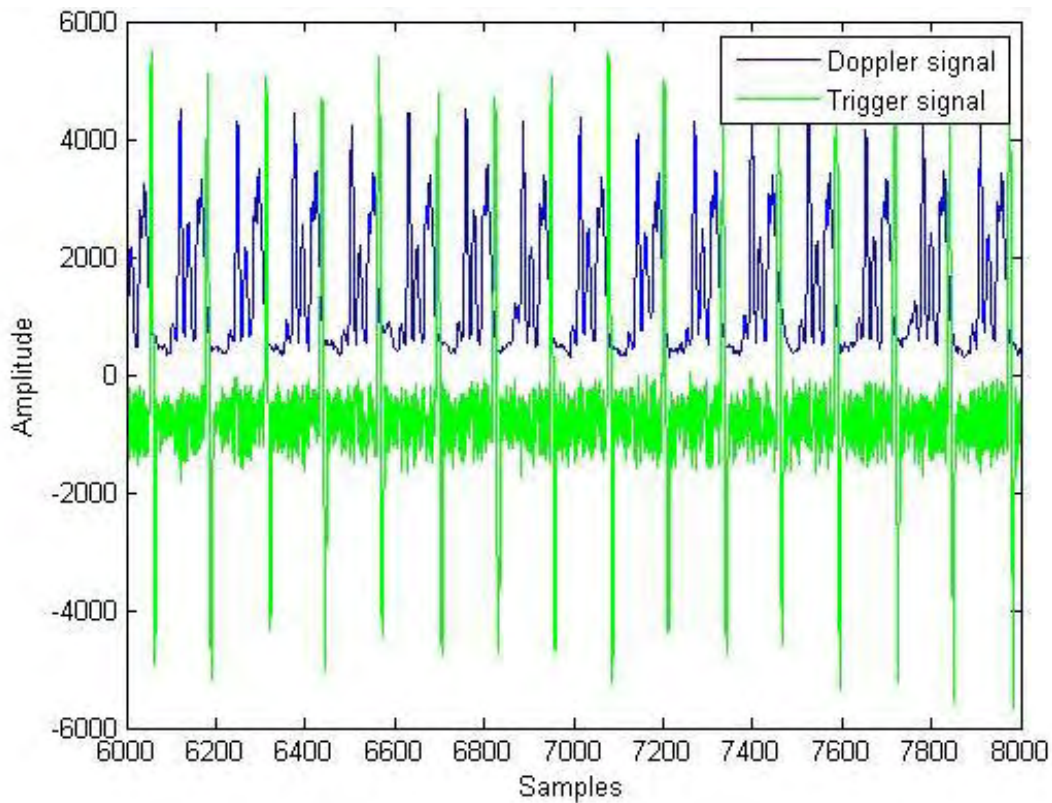
Figure 5.3 Location of trigger signal with respect to Doppler signal for phantom operating at 93 bpm.

5.2.2 Slicing of Balloon

A gradual fall in overall perimeter of a slice was because "V" like shape of balloon construction, as shown in from test 1.
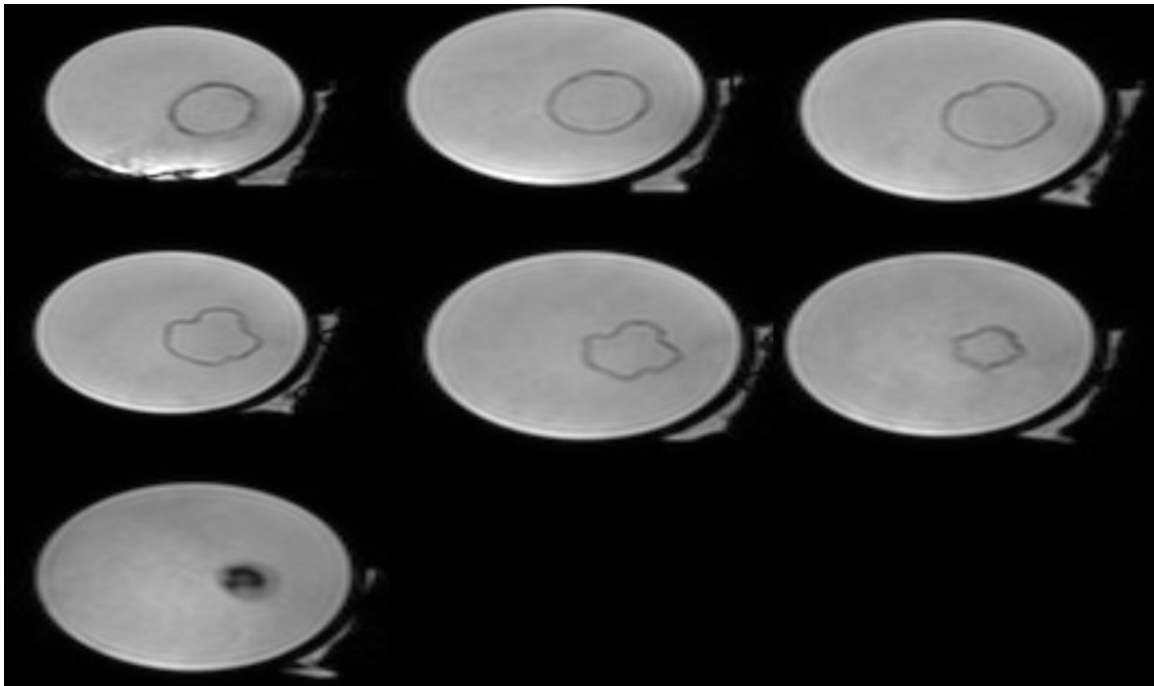
Figure 5.4 Slices of balloon as ventricle at different position. Slice thickness 7mm and 7mm apart.

5.2.3 Comparison of frames

A comparison of equidistant frames for middle slice of balloon, operating at different beats per minute settings. Figure 5.5 shows amount of systole-to-diastole displacement for a middle slice.
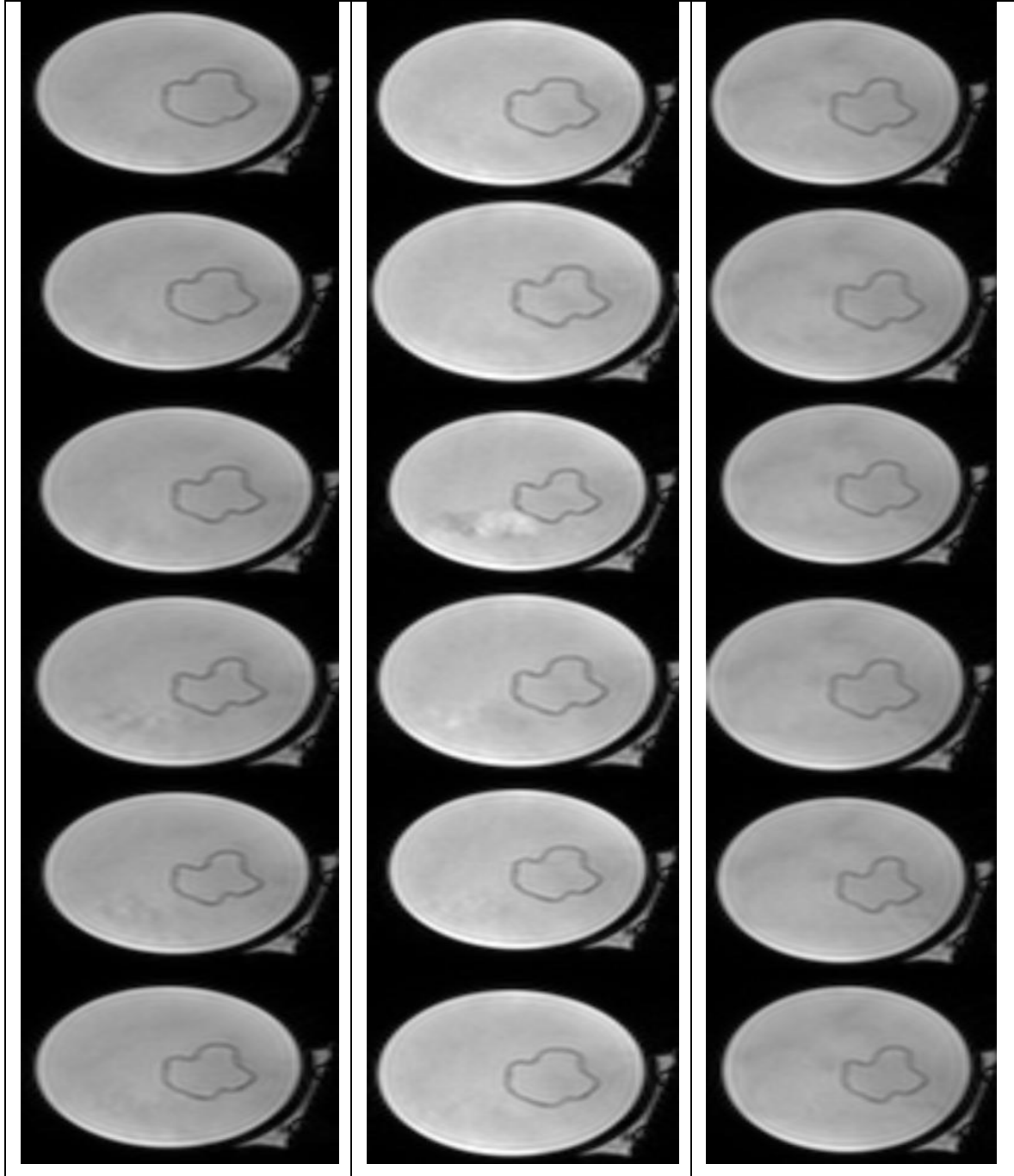
Figure 5.5 Comparison of frames obtained for middle slice at different bpm settings. First column is for 93 bpm, second for 133 bpm and third for 62 bpm. Starting at first frame and an interval of 5 frames in between. Transition from Systole-diastole is visible.

5.2.4   Calculation of stroke volume

Internal Area of balloon for a frame is calculated to using free hand selection function of an image processing software known as ImageJ. Figure 5.6 shows processing of internal area calculation. During imaging cross sectional dimensions were reduced to half. Therefore internal area calculated this is reduced to a factor of 4. Therefore calculated area was 240mm^2 but actual area is 960mm^2. The process is repeated for each frame of each slice. A table listing calculated area is given in Appendix II
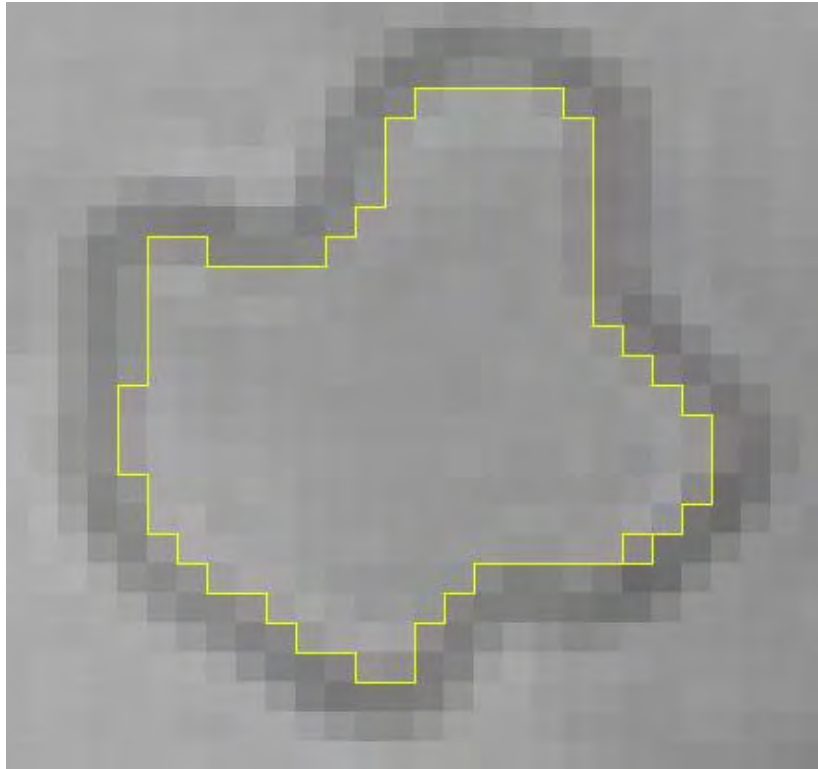
Figure 5.6 Selection of internal region of a balloon using free hand selection function of ImageJ image processing too. Area calculated using this way for this frame was 240 mm^2.

Depth of balloon was 50mm. And we obtain images for 7 slice at 7mm interval and 5 slice at 10 mm interval. And we know that the perimeter for each slice decreases as depth increases. Therefore we use interpolation function in matlab to interpolate data for in between slices approximate 1mm apart. Benefit of having interpolation data of 1mm apart slice is that areas can be added to calculate internal volume of the balloon at that instant. For e.g. using areas of first frame for each slice we can interpolate area of 49 slices slices in between them. By adding areas together total internal volume of balloon can be calculated. Figure 5.7, Figure 5.8, Figure 5.9, Figure 5.10 is demonstrates change in volume of each interpolated slice corresponding to a frame with total maximum and minimum volume.
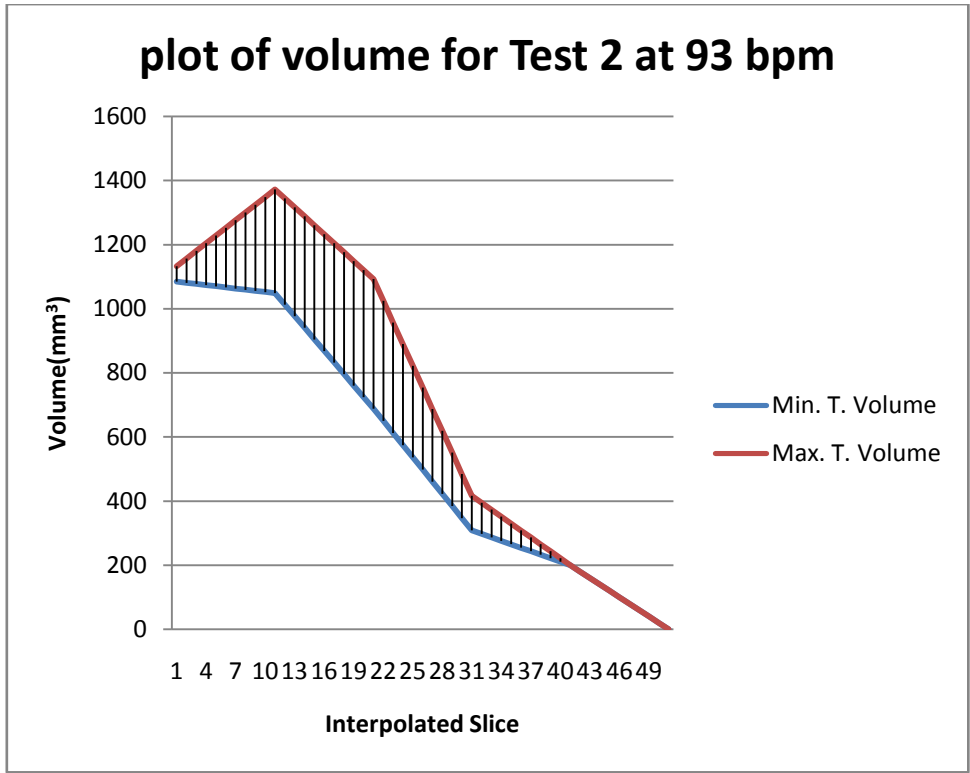
Figure 5.7 Plot of volume of interpolated slices for a frame with total max. volume and that with total min volume.
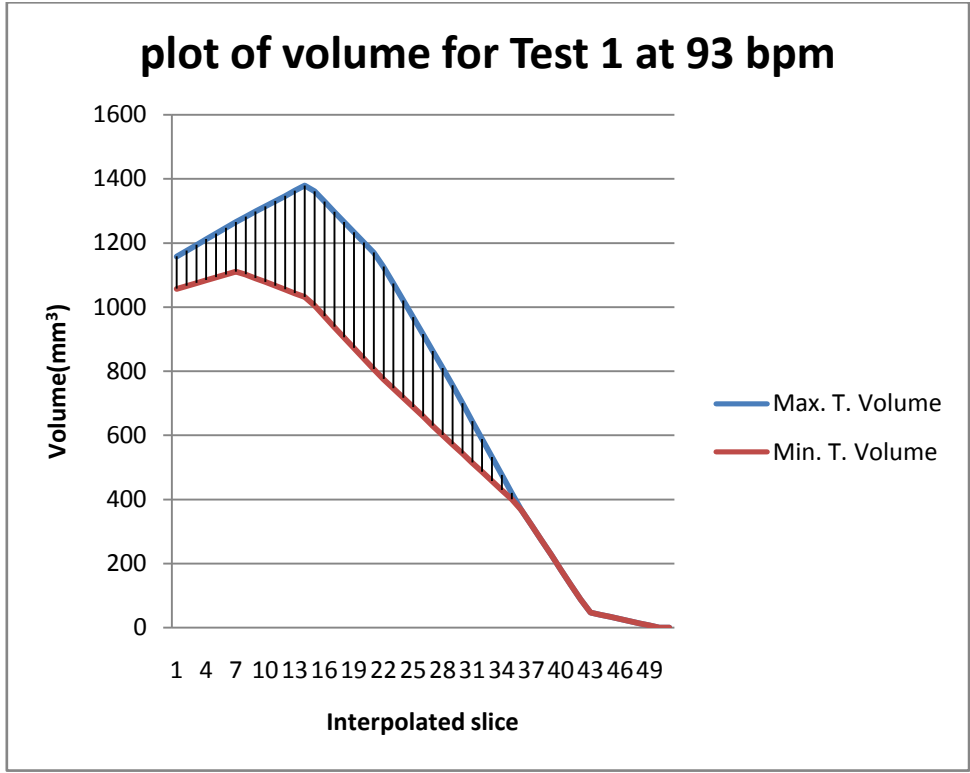
Figure 5.8 Plot of volume of interpolated slices for a frame with total max. volume and that with total min volume.
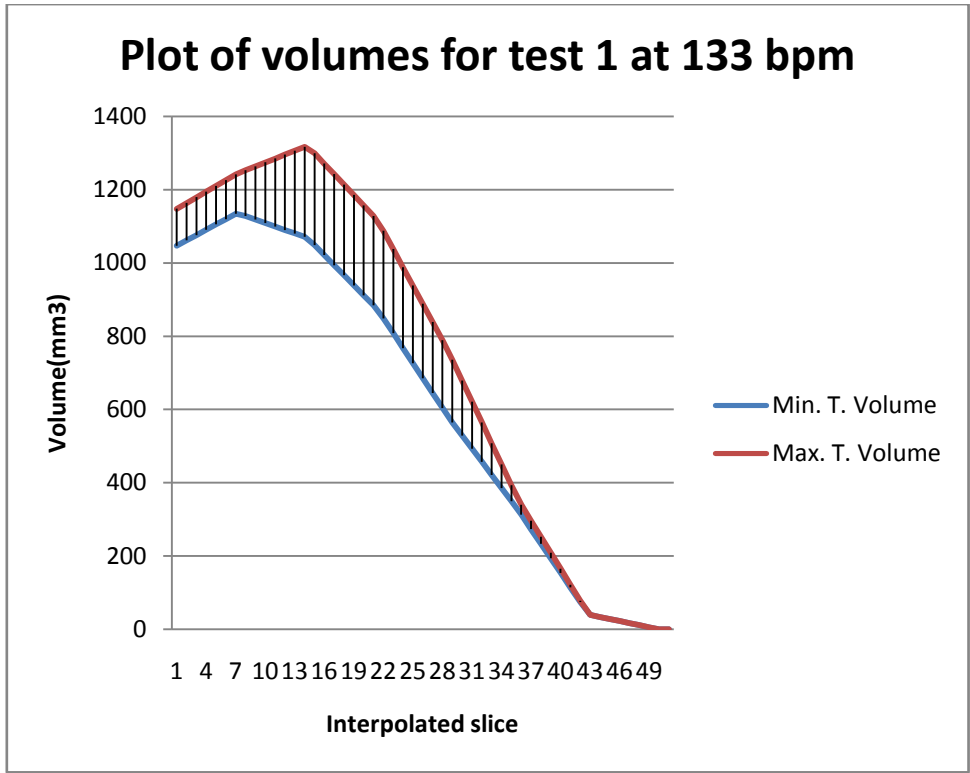
Figure 5.9 Plot of volume of interpolated slices for a frame with total max. volume and that with total min volume.
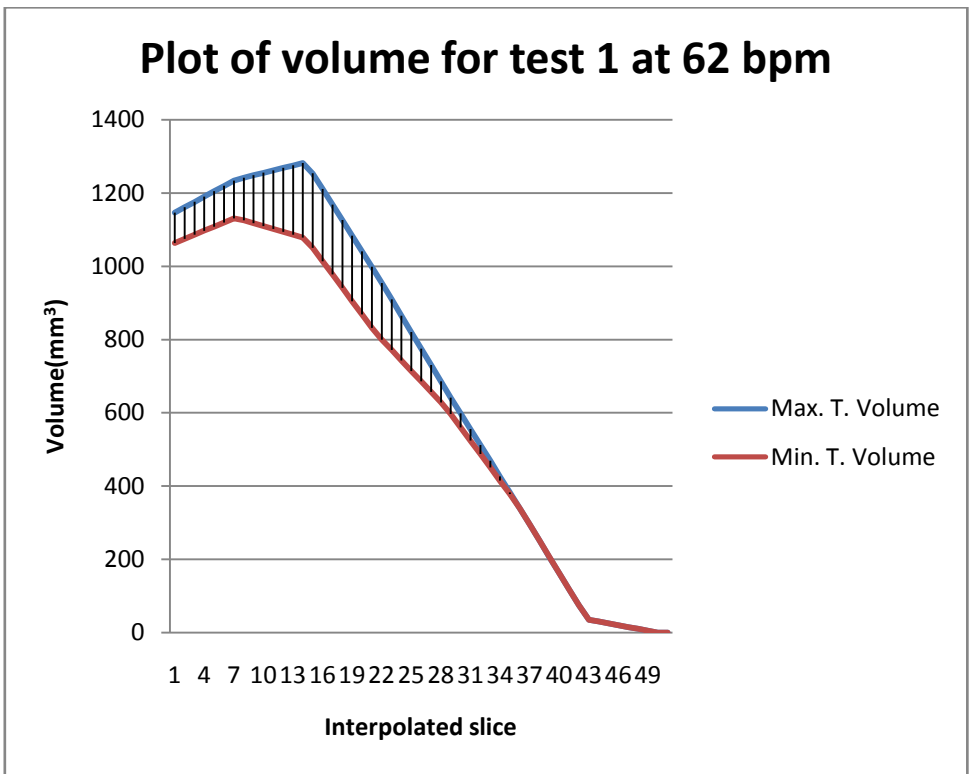
Figure 5.10 Plot of volume of interpolated slices for a frame with total max. volume and that with total min volume.

Calculation of stroke volume with current dimension of balloon shows that it is approximately 4 times more than average stroke volume of a fetal heart as shown in Table 3-1. Figure

Table 5-3 Calculation of Stroke volume

Volume (V)	Test 1			Test 2
	At 62	At 133	At 93	At 93
T. Max.	37091.28	39119.04	40465.44	37026
T. Min.	33023.52	32913.36	32436	28402
ΔV (cu. mm)	4067.76	6205.68	8029.44	8624
ΔV (ml)	4.06776	6.20568	8.02944	8.624

Total volumes over set of 30 corresponding slices were plotted to display pattern of volume change inside balloon, operating at different settings as shown in   Figure   5.11.   By calculating difference between max and min volume, stroke volume can be calculated.
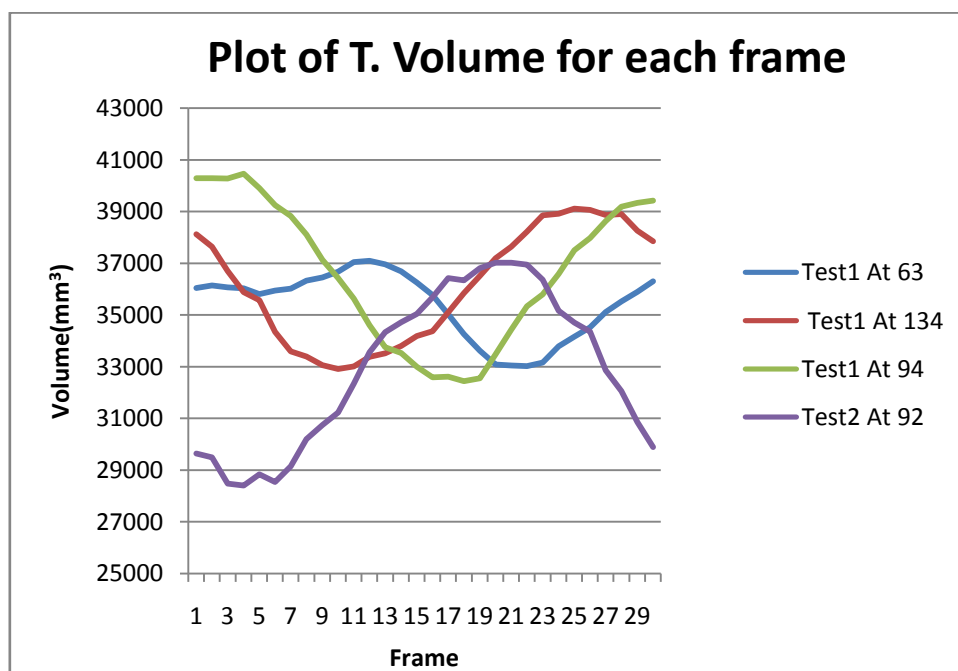
Figure 5.11 Pattern of change in internal volume of balloon operating at different bpm settings.

.

5.2.5   Calculation of Flow rate and Flow velocity

By calculating of the hose through which fluid flows and the flow rate of fluid out of balloon flow velocity of fluid can be calculated. Table 5-4 shows calculation of time interval between max and min total volume of balloon operating at different frequency.

Table 5-4 Calculating time between max. and min. T. Vol.

Test	BPM	Time for each beat (sec)	No. of frames	time interval between frames (sec)	number of frames between max. and min. volume	Total time between max. and min. volume(sec) Δt
Test 1	62	0.967742	30	0.032258	10	0.322581
	133	0.451128	30	0.015038	15	0.225564
	93	0.645161	30	0.021505	14	0.301075
Test 2	93	0.645161	30	0.021505	16	0.344086

Flow rate of fluid flowing in/out of balloon can be calculated using following equation

$$flow\ rate = \frac{\Delta V}{\Delta t} \quad cu.\,mm/sec \tag{5.1}$$

By calculating area of the Silicone pipe through which fluid flows, flow velocity can be calculated. Diameter of Silicone pipe used is 8mm, Therefore,

$$Area\ of\ silicone\ pipe = \frac{\pi \cdot d \cdot d}{4}$$

$$= 50.24\ sq.\,mm$$

Flow velocity of fluid can be calculated by using following formulae.

$$Flow\ velocity = \frac{flow\ rate}{Area\ of\ Silicone\ pipe} \quad mm/\sec \tag{5.2}$$

Table 5-5 Calculation of flow velocity and flow rate

BPM	total time between max and min volume	Stroke volume ΔV (cu. mm)	Flow rate (cu. mm /sec)	Area of 2 Silicone Pipe (sq.mm)	Flow velocity (cm/sec)
62	0.322581	4067.76	12610.06	100.48	12.54982
133	0.225564	6205.68	27511.85	100.48	27.38042
93	0.301075	8029.44	26669.21	100.48	26.54181
93	0.344086	8624	25063.5	100.48	24.94377

6 Test of Phantom with USD

6.1 Method

Figure 6.1 describes setup for phantom used during its testing with Ultra sound Doppler Imaging device. Terason t3000 portable USD is used to measure flow velocity of fluid flowing through the silicone pipe. Linear probe is place over one of the silicone pipe connecting balloon with the reservoir chamber. One of the Silicone hose was blocked temporarily for ease of measurement. Since it is not possible to get scatter signal from a flowing water, water in the phantom was replaced by mustard-sauce thick solution. Granules of mustard scattered US waves and thus flow velocity could be measured.
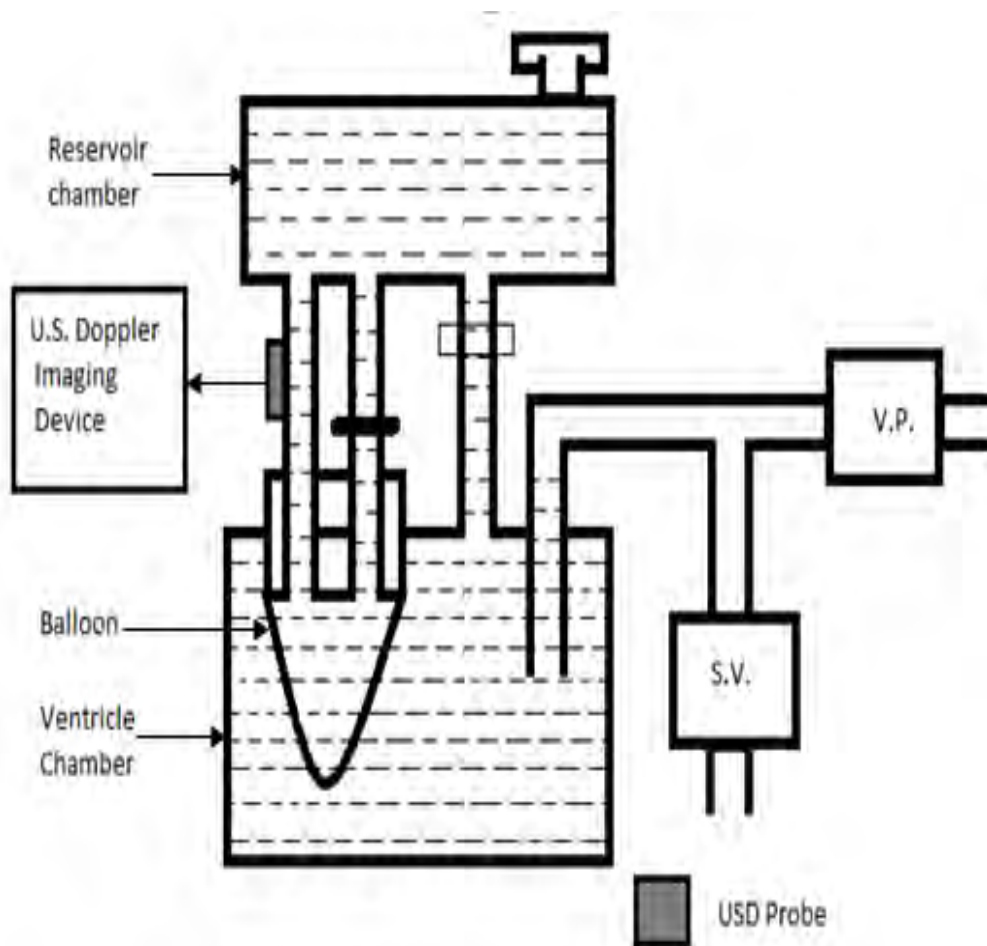
Figure 6.1 Setup for flow velocity measurement using USD

6.2   Results

Initially phantom was testing using low bpm settings, however recorded signal showed aliasing effect. Figure 6.2 Doppler scan of one silicone hose connected to balloon.
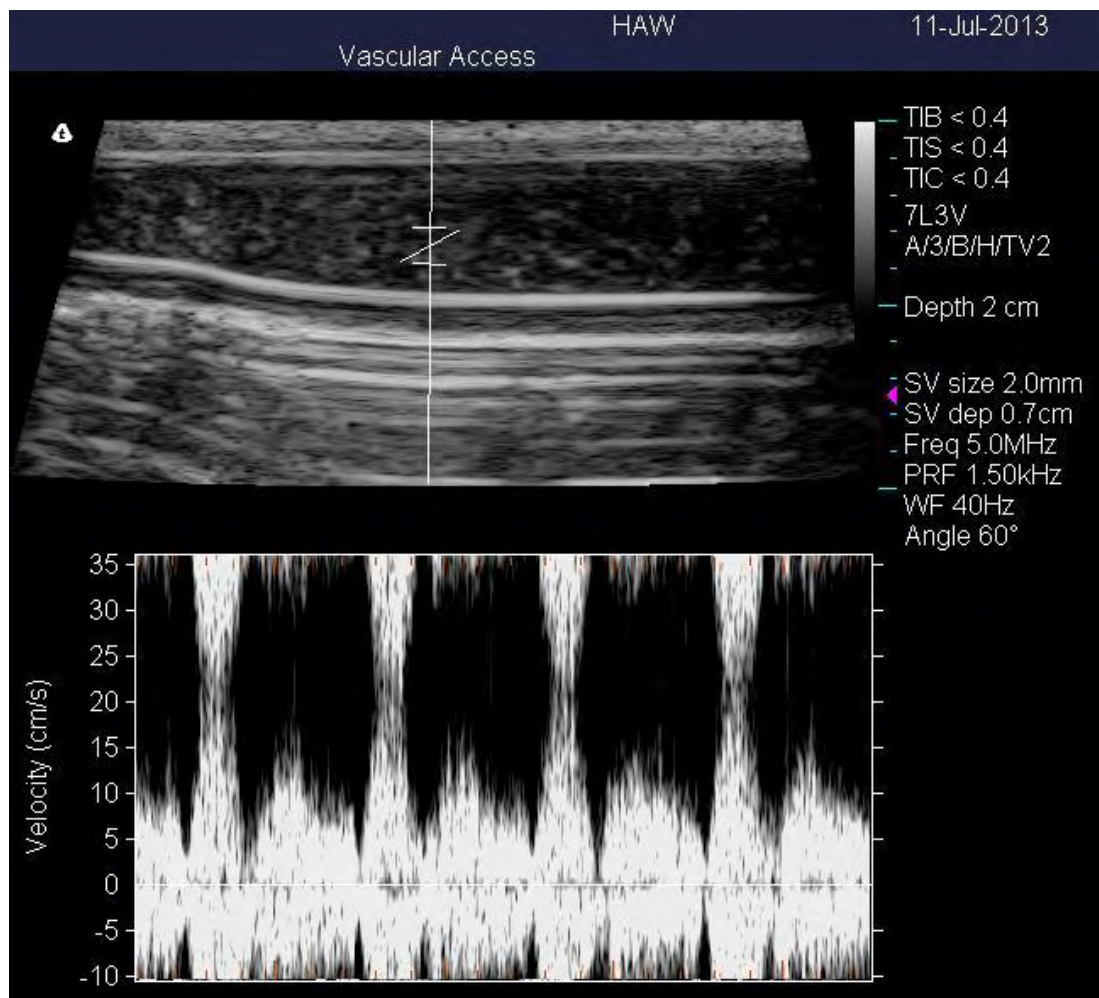
Figure 6.2 Doppler scan of phantom operating at low bpm settings of 62 bpm and duty cycle of 37.5%, with aliasing in recorded signal.

Probable reason for aliasing was having a valve less pipe for connection. Because of this fluid is flowing in both direction with quick reversion in direction of flow. Test conditions were manipulated in order to have some meaningful results. Parameter settings for Control box of phantom are: BPM = 133, Duty cycle of 3.20%, V.P.=2. And blocking one of the silicone pipe. Depth of scan was increased to 80mm by using flexible silicone pads as buffers. Figure 6.3 Improvement in measurement of flow velocity by changing conditions on control box and running phantom at 133 bpm.shows measurements with this changes.
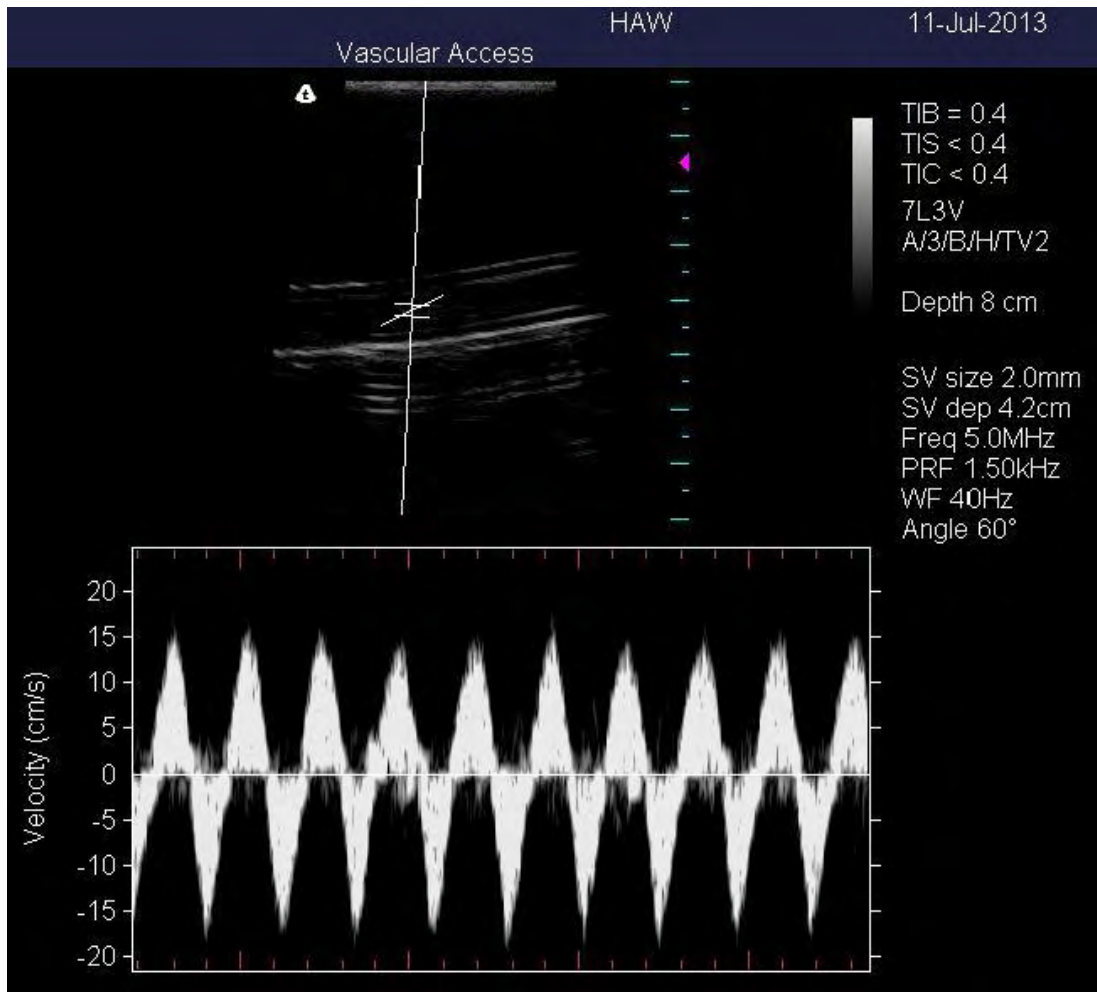
Figure 6.3 Improvement in measurement of flow velocity by changing conditions on control box and running phantom at 133 bpm.

In Figure 6.3 there is an improvement in signal quality, however, to attain this, driving parameters like suction force and duration of suction was compromised. So at this moment no confirmed results could be obtained and used for comparison with calculated flow velocity using MRI images.

7 Discussion and Conclusion

7.1 Discussion

Goal of project was to develop a heart phantom which could be operated successfully under MRI and compatible to ultrasound by providing sufficient frequency shift in transmitted ultrasound waves to be detected by the Transducer used for development of triggering algorithm. To meet this demand a phantom was constructed using simple materials. From repeated experiments using MRI, it was clear that phantom constructed using a simple rubber water balloon worked nicely for Doppler signal acquisition and triggering of MRI system. No artifacts were noticed during or after the tests using phantom. From Figure 5.2 and Figure 5.3 trigger pulse were regular and around local peaks. By controlling parameters like number of operating vacuum pumps amount of systole-diastole displacement was possible to control. Clear visible changes in perimeters of balloon were visible in MRI images.

Conventional method, like use of ultrasound signal, for measuring flow patterns, flow rate, flow velocity of the fluid flowing through connecting pipes were not useful in quantifying these parameters. As shown these in Figure 6.2 signals from fluid flowing in one direction alias with fluid flowing in reverse direction. Therefore these parameters were calculated using another approach, by using images from MRI. Manually calculation of internal area and volume per each slice is prone to human errors. However, it helped in roughly estimating these parameters. Lack of more experimental data limits judgment of accuracy of parameters calculated these way.

In future, use of slightly thick rubber wall for balloon may show improvement in transition from systole to diastole and vice versa. Improvement in size of balloon, design of holder, and accommodation of proper uni-directional valve at the junction on silicone pipe connection will help in developing a model close to left ventricle of fetal heart . Improvement in automation of control box could help in increasing operating range of the phantom.

7.2 Conclusion

Development of a MRI compatible heart phantom opens scope for development of multimodal imaging techniques and helps reducing cost of arranging live test subjects, at least for initial trials. With further improvement in current design, a model very close to Left ventricle of heart can be developed and used as reference body.

Bibliography

1. **Khandpur, R.S.** *Handbook of Biomedical Instrumentation.* New Delhi : Tata McGraw Hill Publishing Company Limited, 2008.

2. **Hoa, Denis.** IMAIOS SAS. *IMAIOS SAS.* [Online] February 15, 2009. http://www.imaios.com/en/e-Courses/e-MRI/Cardiac-MRI/introduction.

3. *A Novel Technique for Cardiac MRI of the Fetal Heart: MR compatible Doppler Ultrasound (CTG) for CardiacTriggering.* **Yamamura J, Frisch M, Kopp I, Graessner J, Hecher K, Adam G, Wedegärtner U.** 2011, Proc. Intl. Soc. Mag. Reson. Med.

4. *Feasibility of MRI of the fetal heart with balanced steady-state free precession sequence along fetal body and cardiac planes.* **SN, Saleem.** 2008, AJR Am J Roentgeno, pp. 1208-1215.

5. *The impact of maternal obesity on mid trimester sonographic visualization of fetal cardiac and craniospinal structures.* **Hendler I, Blackwell SC, Bujold E, et al.** 2004, Int J Obes Relat Metab Disord , pp. 28:1607–1611.

6. *Fetal cardiographic monitoring during 1.5-T MR imaging.* **Michel SC, Rake A, Keller TM, Huch R, König V, Seifert B, Marincek B, Kubik-Huch RA.** 8, s.l. : AJR Am J Roentgenol., 2003, AJR Am J Roentgenol. 180(4), Vol. 180, pp. 1159-1164.

7. *Cardiac MR: Imaging of the Foetal Heart Dynamics using Doppler Ultrasound Triggering.* **Ueberle F, Dettmann E, Eden C, Jayakumar J, Jelinek M, Much C, Schönnagel B, Tavares de Sousa M, Wedegärtner U, Yamamura J.** 2012, Biomed Tech (Berl).

8. *Development and characterization of rodent cardiac phantoms: comparision with in vivo cardiac imaging.* **Steven Fortune, Maurits A. Jansen, Tom Anderson, Gillian A. Gray, Juergen E. Schneider, Peter R. Hoskins, Ian Marshall.** 2012, Magnetic Resonan Imaging, pp. 1186-1191.

9. *Cine Cardiac Imaging Using Black Blood Steady-state free precession(BB-SSFP) at 3T.* **Tamer A. Basha, EL-Sayed H. Ibrahim, Robert G. Weiss, Nael F. Osman.** 2009, Magnetic Resonance Imaging 30, pp. 94-103.

10. *Numerical and In Vivo Validation of Fast Cine Displacement-Encoded with Stimulated Echoes(DENSE) MRI for Quantification of Regional Cardiac Function.* **Li Feng, Rober Donnino, James Babb, Leon Axel, Daniel kim.** 2009, Magnetic Resonance in Medicine 62, pp. 682-690.

11. **Vahid Tavakoli, M.J. Negahdar, Michael Kendrick, Motaz Alshaher, Marcus Stoddard, Amir A. Amini.** A Biventricular Multimodal (MRI/Ultrasound) Cardiac phantom. *IEEE .* Aug-Sept 2012, pp. 3187-3190.

12. *Physiologic Motioin Phantom for MRI Applications.* **Maria Drangova, Brett Bowman, Norbert J. Pelc.** 1996, JMRI 6, pp. 513-518.

13. **W. Paul Segars, David S. Lalush, Eric C. Frey, Dinesh Manocha, Michael A. King, Benjamin M. W. Tsui.** Improved Dynamic Cardiac Phantom Based on 4D NURBS and Tagged MRI. *IEEE Trans Nucl Sci.* 1 October 2009, pp. 2728-2738.

14. *Improved Estimation and Visualization of Two-Dimensional Myocardial Strain Rate Using MR Velocity Mapping.* **Henrik Haraldson, Lars Wigstorm, Magnus Lundberg,**

Ann F. Bolger, Jan Engvall, Tino Ebbers, John-Peder Escobar Kvitting. 2008, Magnetic Resonance Imaging 28, pp. 604-611.

15. *Poly(Vinyl Alcohol) cryogel phantoms for use in ultrasound and MR imaging.* **K.J.M. Surrey, H.J.B. Austin, A. Fenster A, T.M. Peters.** 2004, Phys Med Biol vol. 49, pp. 5529-5546.

16. *Agarose as a tissue equivalent phantom material for NMR imaging.* **Mitchell MD, Kundel HL, Axel L, Joseph PM.** 1986, JMRI vol.4, pp. 263-266.

17. *Characterization of PVA cryogel for intravascular ultrasound elasticity imaging.* **J. Fromageau, E. Brusseau, D. Vray, G. Gimenez and P. Delachartre.** 2003, IEEE Trans Ultrasonic Ferroelectric Freq Control, vol. 10, pp. 1318-1324.

18. *Polyvinyl alcohol cryogel: An ideal phantom material for MR studies of arterial flow and elasticity.* **Rutt, K.C. Chu and B.K.** 1997, Magn Reson Med, vol. 37, pp. 314-319.

19. **Harpell Associates Inc,.** Dynamic Heart Phantom. *Harpell Associates Inc.* [Online] [Cited: 16 July 2013.] http://www.harpell.ca/manufacturer/ptw/dynamic-heart-phantom.

20. **Danielsson, Krissi.** Normal Fetal Heart Rate. *about.com.* [Online] 09 January 2009. [Cited: 03 July 2013.] http://miscarriage.about.com/od/immediatemedicalconcerns/qt/normalfetalhr.htm.

21. **supertech-to-go.com.** Ultrasound Heart Phantom CIRS 067. *supertech-to-go.com.* [Online] [Cited: 16 July 2013.] http://www.supertech-to-go.com/ulheph.html.

22. **Shelley Medical Imaging Technologies.** Dynamic Heart Phantoms, Multi-Modal. *Shelley Medical Imaging Technologies.* [Online] [Cited: 16 July 2013.] http://www.simutec.com/dynamic_hearts.html.

23. **Raymond Chan, Robert Manzke, Douglas A. Stanton, Guy shechter.** *Anatomically and functionally accurate soft tisse phantoms and method for generation.* s.l. : United States Patent Application Publication, 2010.

24. **Boston Children's Hospital.** Fetus and Newborn blood circulation. *Boston Children's Hospital.* [Online] [Cited: April 4, 2013.] http://www.childrenshospital.org/az/Site636/mainpageS636P0.html.

25. *Fetal cardiac stroke volume determination by four-dimensional ultrasound with spatio-temporal image correlation compared with two-dimensional and Doppler ultrasonography.* **Giuseppe Rizzo, Alessandra Capponi Ottavia Cavicchioni, Marianne Vendola and Domenico Arduini.** 2007, PRENATAL DIAGNOSIS, pp. 27: 1147–1150.

26. **Noll, Douglas C.** *A Primer on MRI and Functional MRI.* 2001.

27. **Jason Wang, Michael Asensio.** MRI Theory. *University of Illinois, College of Engineering.* [Online] 15 December 2010. [Cited: 16 July 2013.] https://wiki.engr.illinois.edu/display/BIOE414/MRI+Theory.

28. Fetal ECG Extraction using LabVIEW. *National Instruments Developer zone.* [Online] 8 May 2013. [Cited: 01 07 2013.] http://www.ni.com/white-paper/11248/en/.

29. *Influence of the maternal ECG on the abdominal fetal ECG complex.* **van Bemmel JH, Peeters L, Hengeveld SJ.** 1968, American Journal of Obstetrics and Gynecology, pp. 102,556.

30. *Noise Reduction in fetal electrocardiography, II: Averaging Technique.* **Lee, E.H. Hon and S. T.** 1964, Medical electronics and biological engineerign, pp. 71-76.

31. *Systolic Fetal Heart Murmur Detected in Fetal Phonocardiography.* **Maeda K, Nakano H.** 2013, Occupational Medicine and Health Affairs, p. 1:102.

32. **Bertolina, Michael.** The doppler phone. *Open Ideo.* [Online] 14 March 2011. [Cited: 04 July 2013.] http://www.openideo.com/open/maternal-health/concepting/the-doppler-phone.

33. mini vacuum pump. *ebay.* [Online] 8 june 2013. [Cited: 24 june 2013.] http://www.ebay.de/itm/Mini-Vakuumpumpe-mini-12V-2L-min-Vakuum-pumpe-Saugpumpe-12-Volt-/251250766834.

34. Bausatz Stepdown-Wandler. *Pollin electronics.* [Online] [Cited: 8 July 2013.] http://www.pollin.de/shop/dt/ODc4OTgxOTk-/Bausaetze_Module/Bausaetze/Bausatz_Stepdown_Wandler.html.

35. Solenoid-valve-info. *Solenoid-valve-info.* [Online] [Cited: 26 06 2013.] http://www.solenoid-valve-info.com/solenoid-valve-definition.html.

36. **Mugal, Sami.** Creating a variable Frequency PWM output on Arduino UNO. *Oxgadgets.* [Online] 7 04 2011. [Cited: 28 12 2012.] http://www.oxgadgets.com/2011/04/creating-a-variable-frequency-pwm-output-on-arduino-uno.html.

37. Duckbill valves. *mini valve.* [Online] minivalve international. [Cited: 08 july 2013.] http://minivalve.com/newsite/index.php/en/by-type/duckbill-valves/how-they-work.

Appendix I   Design of phantom with valves

Figure 0.1 show a phantom enclosed in an acrylic box, filled with water. Two unidirectional valves fitted on balloon-valve holder. They were glued in opposite direction using hot silicone glue stick. Figure 0.2shows Ø12mm Duckbill type of valve used for this purpose (37). Figure 0.3 shows it's working (37). A duckbill valve has two lips. Which opens in one direction of flow and seals itself when the direction of flow reverses.
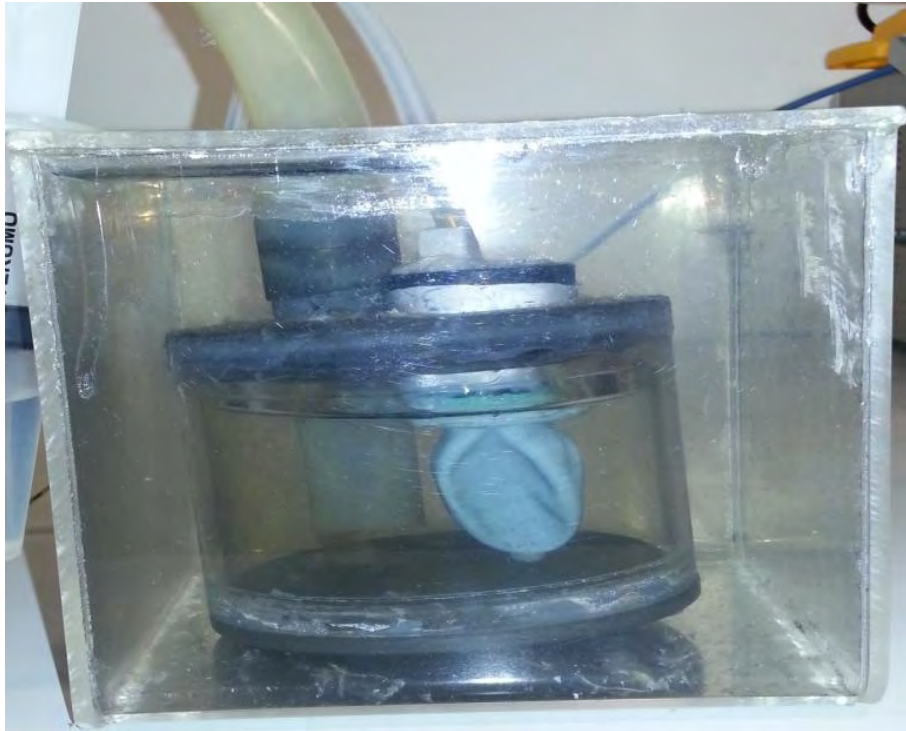
Figure 0.1 **Phantom with valves and placed in a closed acrylic box**

Figure 0.2 **Uni-directional mini valve(duckbill type)**
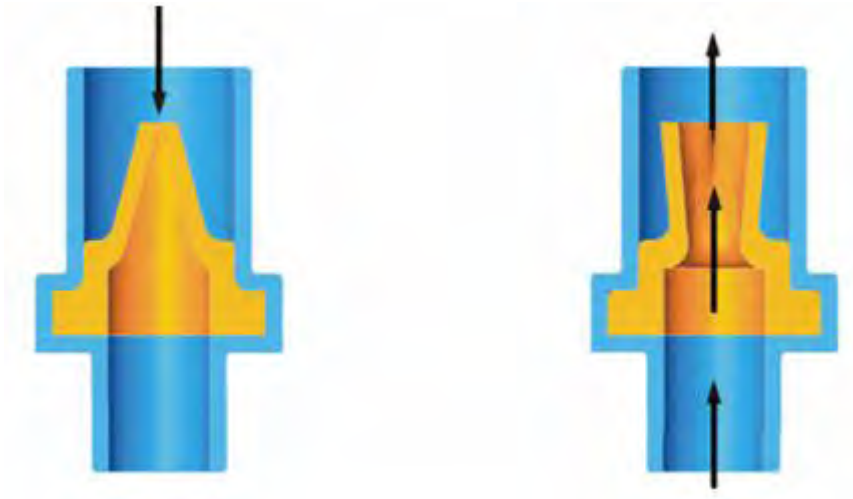
Figure 0.3 Working of Duckbill valve.

Appendix II   Table of internal area of balloon

Freehand area calculation using ImageJ for every frame.

Table 0-1 From test1 at 93 bpm

Slice 1	Slice 2	Slice 3	Slice 4	Slice 5	Slice 6	Slice 7
290	319	344	285	190	95	12
281	322	343	285	193	95	12
284	320	343	289	189	95	12
285	317	346	289	195	95	12
291	315	336	282	191	95	12
291	312	333	270	186	95	12
283	313	322	273	183	95	12
284	312	316	258	179	95	12
277	309	307	246	173	95	12
281	306	298	238	166	95	12
276	303	294	230	156	95	12
271	303	278	222	147	95	12
269	293	274	211	143	95	12
266	286	267	217	145	95	12
267	282	257	213	144	95	12
270	277	255	209	139	95	12
266	284	259	197	143	95	12
262	278	257	198	146	95	12
267	273	258	204	145	95	12
270	283	267	208	153	95	12
278	288	274	218	160	95	12
277	293	285	230	164	95	12
282	293	291	230	171	95	12
289	294	297	243	175	95	12
289	300	309	252	180	95	12
290	308	311	257	181	95	12
290	314	321	261	184	95	12
289	316	330	266	188	95	12
289	308	334	269	194	95	12
288	304	340	274	191	95	12

Table 0-2 From test1 at 133

Slice 1	Slice 2	Slice 3	Slice 4	Slice 5	Slice 6	Slice 7
283	317	320	257	181	88	10
282	311	315	252	181	88	10
273	307	305	242	177	88	10
267	304	291	240	171	88	10
265	302	291	235	168	88	10
267	295	283	231	150	81	10
263	294	276	222	143	81	10
261	287	275	220	147	81	10
265	281	271	218	145	81	10
258	284	267	218	145	81	10
255	281	271	217	150	81	10
262	279	271	222	156	81	10
258	281	272	225	157	81	10
260	282	275	226	161	81	10
264	288	281	225	161	81	10
265	288	279	230	164	81	10
271	291	290	232	170	81	10
277	297	298	236	170	86	10
274	303	301	246	176	86	10
277	309	307	252	180	86	10
275	306	319	257	183	86	10
279	311	325	262	183	88	10
281	312	336	268	186	88	10
279	312	336	270	187	88	10
283	311	330	279	190	88	10
283	311	331	276	190	88	10
278	311	331	272	190	88	10
277	314	331	270	191	88	10
269	311	324	267	186	88	10
270	311	322	256	184	88	10

Table 0-3 From test1 at 62

Slice 1	Slice 2	Slice 3	Slice 4	Slice 5	Slice 6	Slice 7
282	307	298	240	161	86	9
279	305	300	239	165	88	9
276	306	300	238	166	86	9
272	305	301	237	166	88	9
271	304	302	231	166	87	9
272	306	303	234	163	88	9
273	307	303	235	164	87	9
275	309	307	236	166	88	9
275	310	311	238	165	86	9
277	312	311	242	165	87	9
282	312	314	248	165	88	9
283	309	321	245	165	88	9
284	310	318	242	165	88	9
281	310	308	241	168	88	9
279	310	302	236	166	87	9
279	307	294	230	166	87	9
274	299	289	223	162	88	9
274	296	279	210	162	87	9
271	290	266	208	162	87	9
267	287	263	203	157	87	9
266	285	266	202	155	88	9
263	283	269	204	153	88	9
266	287	268	205	152	88	9
268	287	276	216	154	88	9
266	291	282	219	155	88	9
269	292	287	225	154	88	9
272	296	295	231	155	88	9
273	301	298	232	160	88	9
278	303	300	237	161	88	9
282	307	304	240	162	88	9

Table 0-4 From Test 2 at 93 bpm

Slice 1	Slice 2	Slice 3	Slice 4	Slice 5
280	283	181	73	50
277	280	179	76	50
271	266	171	76	50
271	262	172	77	50
267	263	174	87	50
261	264	178	78	50
263	271	182	81	50
267	275	196	87	50
274	281	200	87	50
276	293	201	85	50
281	299	212	93	50
287	314	219	98	50
290	327	227	95	50
287	336	233	91	50
282	342	237	92	50
284	341	249	96	50
285	350	257	97	50
281	350	262	92	50
284	350	266	98	50
283	343	273	104	50
283	340	277	103	50
283	343	277	98	50
282	346	263	95	50
280	338	255	82	50
281	340	237	86	50
282	342	234	78	50
279	330	217	71	50
279	316	209	73	50
279	292	201	75	50
275	290	190	66	50

Appendix III   Projection Drawing

a) Acrylic pipe
b) Bottom cover
c) Top cover
d) Balloon and Valve holder
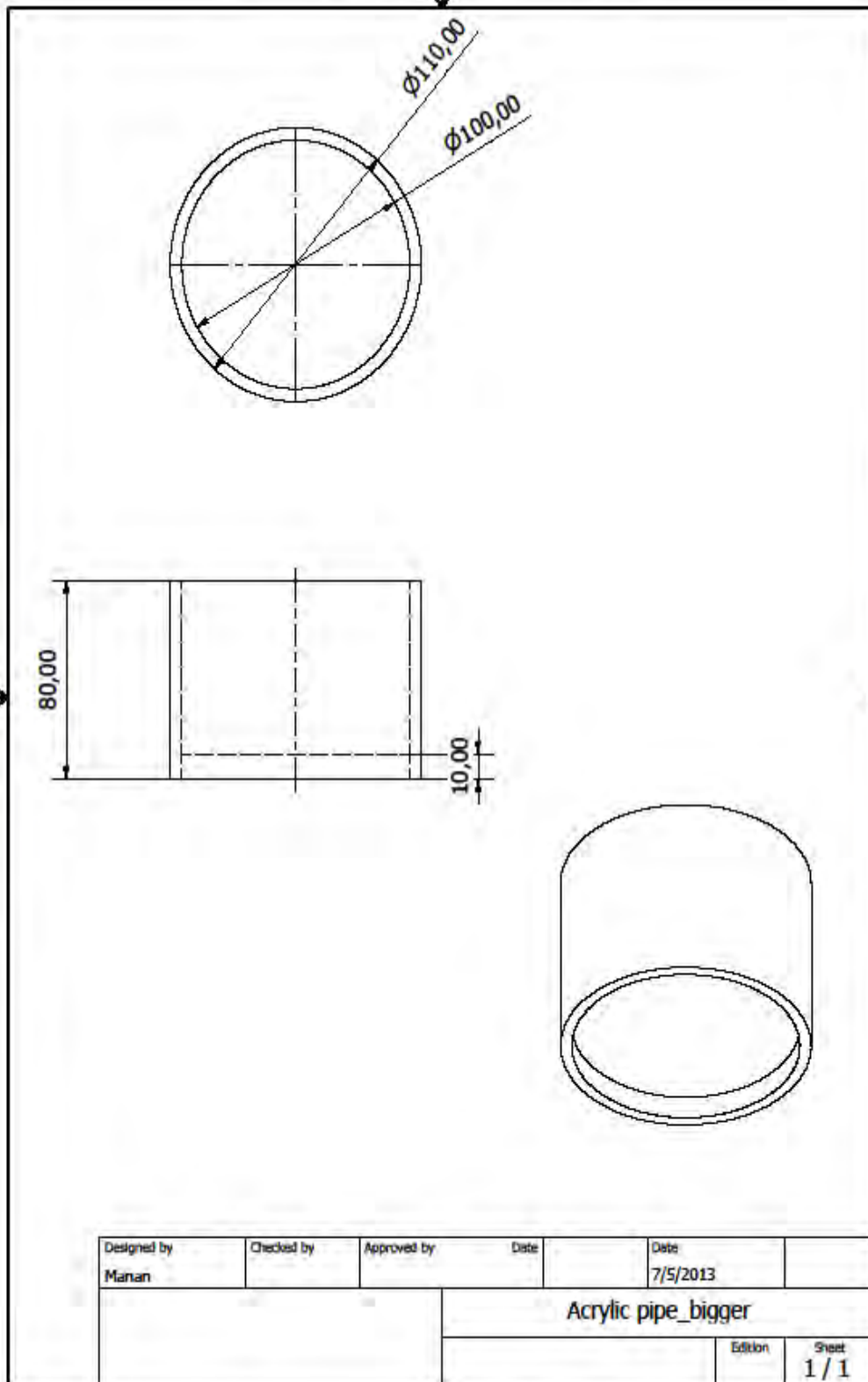
Ø110,00

Ø100,00

80,00

10,00

Designed by	Checked by	Approved by	Date		Date	
Manan					7/5/2013	
			Acrylic pipe_bigger			
					Edition	Sheet
						1 / 1

Ø110,00

Ø100,00

50,00
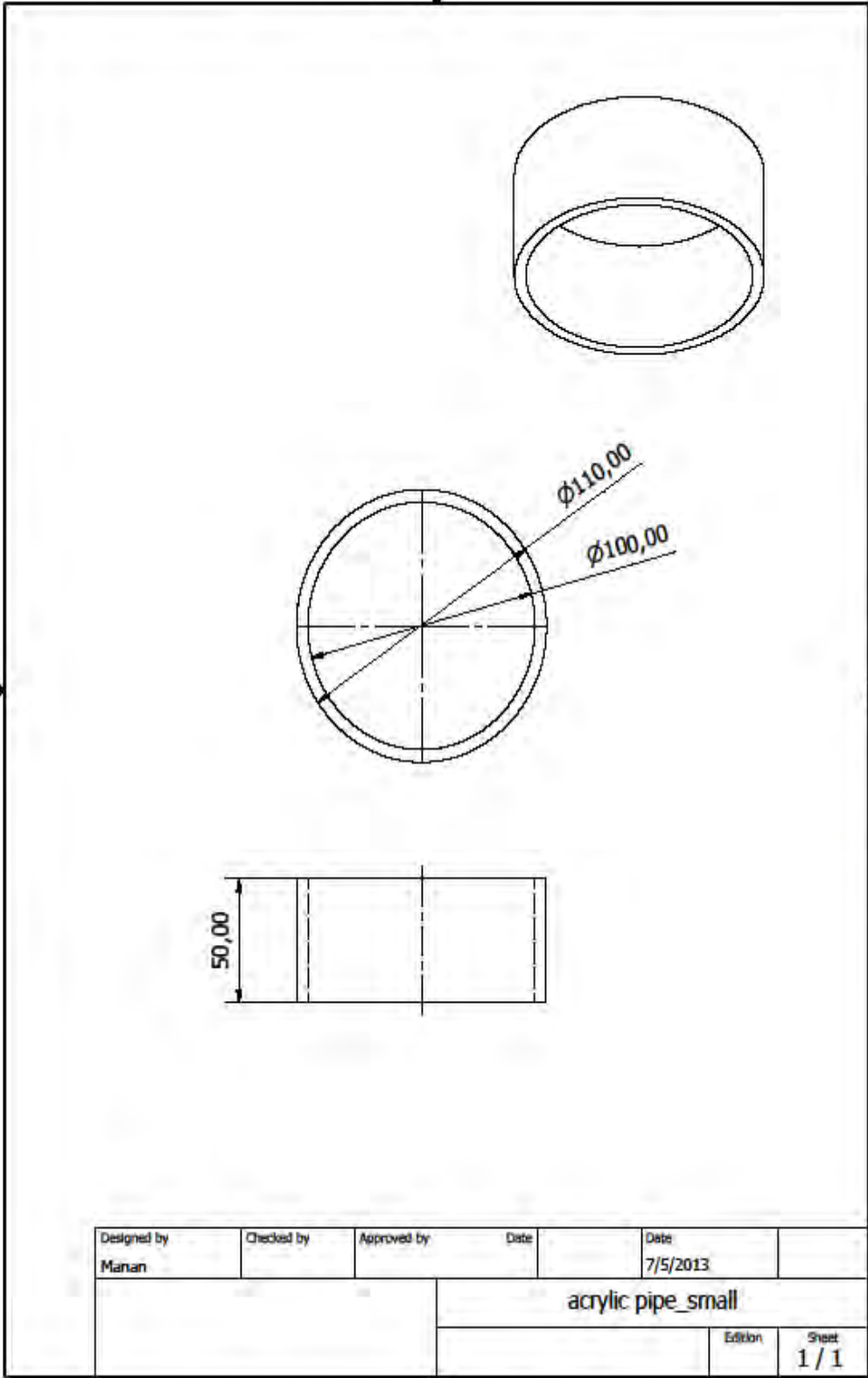
Designed by	Checked by	Approved by	Date		Date	
Manan					7/5/2013	
			acrylic pipe_small			
					Edition	Sheet
						1 / 1

10,00

5,00

Ø110,00

Ø100,00
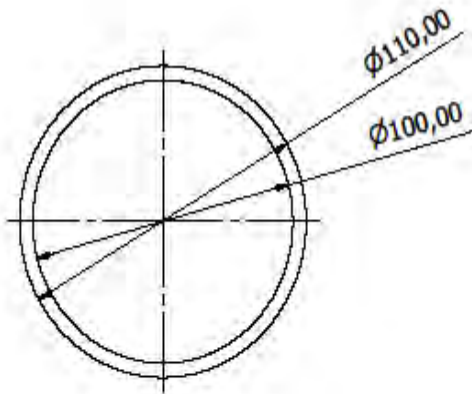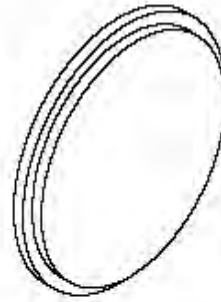
Designed by	Checked by	Approved by	Date		Date	
Manan					7/5/2013	

bottom cover

	Edition	Sheet
		1 / 1

X

Ø28,00
Ø100,00
Ø110,00
Ø36,00

B   B

M36x2 - 6H

B-B (1 : 1)

15,00
5,00

5,00
20,00
34,00
72,00

C
C (2 : 1)

Nut fuer
O ring
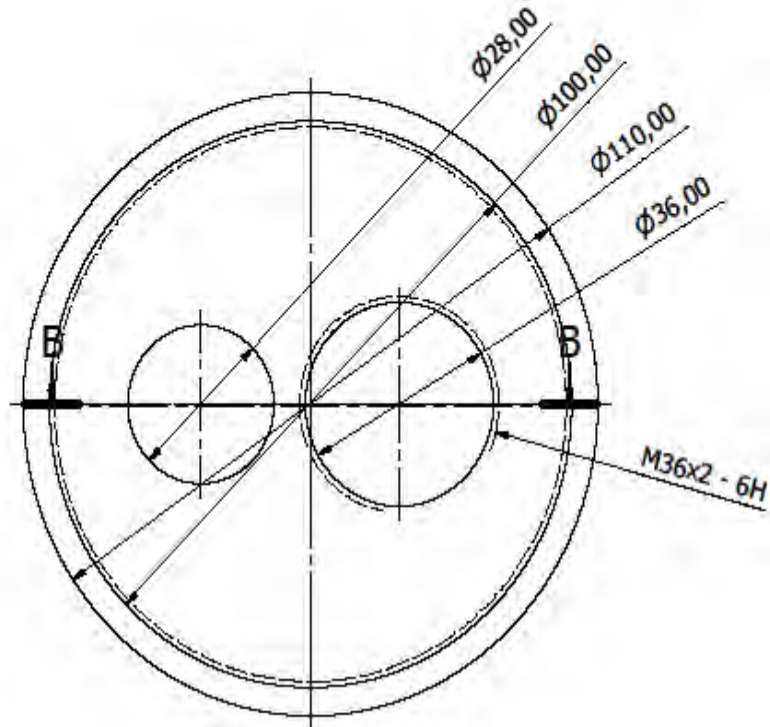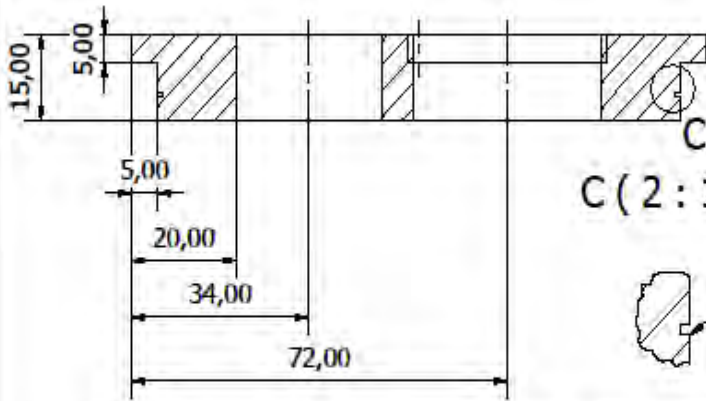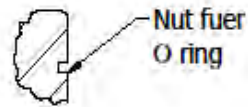
Designed by	Checked by	Approved by	Date	Date	
Manan				7/5/2013	

top cover

deckel4 · Edition · Sheet 1 / 1

Ø41,00
Ø36,00
Ø33,00
Ø12,00
Ø12,00
M33x2 - 6g LH

12,00
15,00
42,00
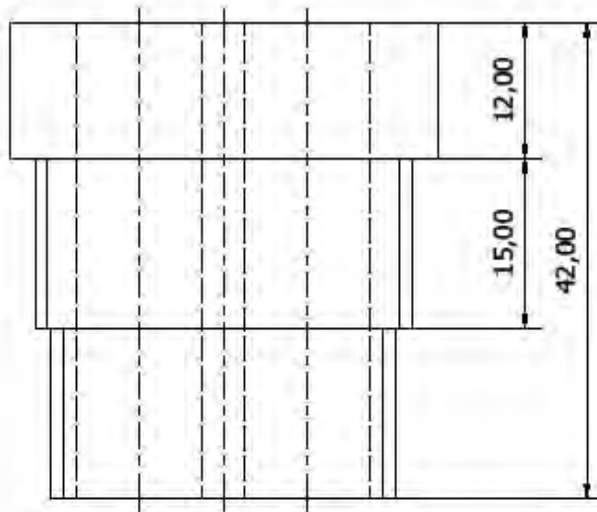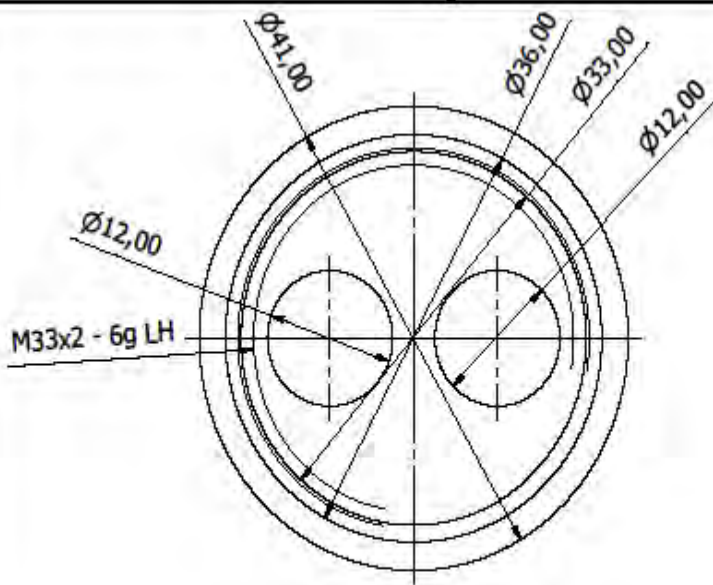
Designed by	Checked by	Approved by	Date	Date	
Manan				7/5/2013	

balloon-valve holder

Edition | Sheet
1 / 1

Appendix IV   C code for Arduino Uno

```
/*********************** C Code for ARDUINO  UNO ATmega328P
**************/
/* Two POTS are connected over two ananlog pins of Arduino UNO board.
 A POT connected to  Analog pin A3 will be used for controlling pulse frequency
 A POT connected to  Analog pin A4 will be used for controlling PWM of the pulse.
 Timer 1 is used for pulse generation.
*/

// Include header files.
// including header file for LCD display.
#include<LiquidCrystal.h>

// declaration of global variables.
long  bpm_pot; // variable for storing bpm value
float pwm_pot; // variable for storing read value of pot used for PWM

/* setup function will perform following tasks:
        a. configuring PWM pins as output
        b. defining mode of Timer/counter control registers.
        c. clock division factor
        d. LCD setup.
*/
void setup()
{
        // set pin 9 as pulse output mode.
        pinMode(9,OUTPUT);

        // set timer/counter control register A to mode 8
        // mode 8 is for phase frequency correct mode.
        TCCR1A = _BV(COM1A1) | _BV(COM1B1);

        // set clock select bits of timer/counter control register B
        // to 1024.
        TCCR1B = _BV(WGM13) | _BV(CS12) | _BV(CS10);

        // set up the LCD's number of columns and rows.
        // we use 16*2 type LCD for display.
        LCD.begin(16,2);
}


/* now we enter into infinite loop and do following tasks.
        a. read analog channel A3 for setting frequency of the pulse generated.
        b. read A3 and set value in Input Capture Register ICR1
        c. read A4 and set appropriate value of Output control register for PWM.
        d. display BPM and PWM value.
*/
void loop()
```

```
{
        // ICR1 value for getting 39 beats per minute.
        if(analogRead(A3) < 50)
        {
                ICR1 = 12000;
                bpm_pot = 39;
        }

        // ICR1 value for getting 40 beats per minute.
        if(analogRead(A3) < 100 && analogRead(A3) > 50)
        {
                ICR1 = 11500;
                bpm_pot = 40;
        }

        // ICR1 value for getting 42 beats per minute.
        if(analogRead(A3) < 150 && analogRead(A3) > 100)
        {
                ICR1 = 11000;
                bpm_pot = 42;
        }

        // ICR1 value for getting 44 beats per minute.
        if(analogRead(A3) < 200 && analogRead(A3) > 150)
        {
                ICR1 = 10500;
                bpm_pot = 44;
        }

        // ICR1 value for getting 46 beats per minute.
        if(analogRead(A3) < 250 && analogRead(A3) > 200)
        {
                ICR1 = 10000;
                bpm_pot = 46;
        }

        // ICR1 value for getting 49 beats per minute.
        if(analogRead(A3) < 300 && analogRead(A3) > 250)
        {
                ICR1 = 9500;
                bpm_pot = 49;
        }

        // ICR1 value for getting 52 beats per minute.
        if(analogRead(A3) < 350 && analogRead(A3) > 300)
        {
                ICR1 = 9000;
                bpm_pot = 52;
        }
```

```
// ICR1 value for getting 55 beats per minute.
if(analogRead(A3) < 400 && analogRead(A3) > 350)
{
        ICR1 = 8500;
        bpm_pot = 55;
}

// ICR1 value for getting 59 beats per minute.
if(analogRead(A3) < 450 && analogRead(A3) > 400)
{
        ICR1 = 8000;
        bpm_pot = 59;
}

// ICR1 value for getting 62 beats per minute.
if(analogRead(A3) < 500 && analogRead(A3) > 450)
{
        ICR1 = 7500;
        bpm_pot = 62;
}

// ICR1 value for getting 67 beats per minute.
if(analogRead(A3) < 550 && analogRead(A3) > 500)
{
        ICR1 = 7000;
        bpm_pot = 67;
}

// ICR1 value for getting 72 beats per minute.
if(analogRead(A3) < 600 && analogRead(A3) > 550)
{
        ICR1 = 6500;
        bpm_pot = 72;
}

// ICR1 value for getting 78 beats per minute.
if(analogRead(A3) < 650 && analogRead(A3) > 600)
{
        ICR1 = 6000;
        bpm_pot = 78;
}

// ICR1 value for getting 85 beats per minute.
if(analogRead(A3) < 700 && analogRead(A3) > 650)
{
        ICR1 = 5500;
        bpm_pot = 85;
}

// ICR1 value for getting 93 beats per minute.
```

```
        if(analogRead(A3) < 750 && analogRead(A3) > 700)
        {
                ICR1 = 5000;
                bpm_pot = 93;
        }

        // ICR1 value for getting 104 beats per minute.
        if(analogRead(A3) < 800 && analogRead(A3) > 750)
        {
                ICR1 = 4500;
                bpm_pot = 104;
        }

        // ICR1 value for getting 117 beats per minute.
        if(analogRead(A3) < 850 && analogRead(A3) > 800)
        {
                ICR1 = 4000;
                bpm_pot = 117;
        }

        // ICR1 value for getting 133 beats per minute.
        if(analogRead(A3) < 900 && analogRead(A3) > 850)
        {
                ICR1 = 3500;
                bpm_pot = 133;
        }

        // ICR1 value for getting 156 beats per minute.
        if(analogRead(A3) < 950 && analogRead(A3) > 900)
        {
                ICR1 = 3000;
                bpm_pot = 156;
        }

        // ICR1 value for getting 187 beats per minute.
        if(analogRead(A3) < 1000 && analogRead(A3) > 950)
        {
                ICR1 = 2500;
                bpm_pot = 187;
        }

        // returning back to 72 bpm if pot cross a certain high point.
        if(analogRead(A3) > 1000)
        {
                ICR1 = 6500;
                bpm_pot = 72;
        }

// once the pulse frequency is set we can adjust Pulse width of pulses.
        // read analog value on A4
```

```
        // convert into float
        pwm_pot = float(analogRead(A4));

// converting pwn_pot to proper percentage value
        pwn_pot = pwn_pot*ICR1;
        pwm_pot = pwn_pot/1023;

// assigning value to OCR register.
        OCR1A = int(pwm_pot);

        // clear LCD display
        lcd.clear();
        // position cursor to 0,0 position
        lcd.setCursor(0,0);
        // printing a message
        lcd.print("*Heart Phantom.*");

        // moving to second line
        lcd.setCursor(0,2);
        lcd.print("Bpm:");

        // printing bpm value
        lcd.print(bpm_pot);

        // reading and printing PWM value.
        lcd.print(" Pwm:");
        lcd.print((float(analogread(A4)))/10);

        // wait for 0.5 sec and then repeat above process.
        delay(500);

}
```